

DMAW 2010 LEGACY

the Presentation Review:

Dark Matter in Galaxies

with its Explanatory Notes

Paolo Salucci¹, Christiane Frigerio Martins², and Andrea Lapi³

¹SISSA/ISAS, via Bonomea 265, 34136 Trieste, Italy

²INFES/Univ. Federal Fluminense, av. João Jazbik, 28470 Santo Antônio de Pádua, RJ, Brazil

³Dip. Fisica, Univ. di Roma "Tor Vergata", Via Ricerca Scientifica 1, 00133 Roma, Italy

With the scientific collaboration of Elena Aprile, Mariangela Bernardi, Albert Bosma, Erwin de Blok, Ken Freeman, Refael Gavazzi, Gianfranco Gentile, Gerry Gilmore, Uli Klein, Gary Mamon, Claudia Maraston, Nicola Napolitano, Pierre Salati, Chiara Tonini, Mark Wilkinson, Irina Yegorova.

With the support and encouragement of A. Burkert, J. Bailin, P. Biermann, A. Bressan, S. Capozziello, L. Danese, C. Frenk, S. Leach, M. Roos, V. Rubin

1 General Introduction

The Journal Club Talk "Dark Matter in Galaxies" was delivered within the "Dark Matter Awareness Week (1-8 December 2010)" at 140 institutes in 46 countries and was followed by 4200 people. More information on DMAW can be found at its website: www.sissa.it/ap/dmg/index.html and a short movie that documents this worldwide initiative at: <http://www.youtube.com/watch?v=A0Bit8a-1Fw>.

For this DMAW 2010 talk there was a standard reference presentation with explaining notes prepared by a coordinated pool of leading scientists in the field, which the various speakers adapted and delivered in their Institutes so as to suit local circumstances, audiences and their own personal preferences. Importantly, the speakers subsequently provided us with comments on the reference material and on the initiative itself (see Section 1.3 to download them).

After the event, in response to participants' feedback, we improved and upgraded the guideline material to a "Presentation Review" on the subject "Dark Matter in Galaxies", for which we provide a .pptx file and the related Explanatory Notes. This is described below together with suggestions of who might be interested in using it and how to do it.

1.1 What is the Presentation Review + Explanatory Notes?

This is an innovative scientific product, introduced for fostering scientific debate on Cosmology and for rapidly diffusing, among the scientific community, results in a field where, we believe, knowledge is rapidly growing. Supported by the large number of speakers delivering the DMAW 2010 talk, by their reactions and by those of their numerous audiences, we decided to address the whole community

of cosmologists and astrophysicists. We prepared this Presentation Review, convinced that there is a generalized request of knowledge about the DM mystery at galactic scale.

The Presentation is a Review Talk at post-graduate level, (2 x 45) minutes long, on the specific subject: "The distribution of Dark (and Luminous) Matter in Galaxies", although other cosmological issues (e.g. galaxy formation) are treated, but from the phenomenological perspective of the galaxy mass distribution.

The Presentation Review is not a PowerPoint translation of an already existing Review Paper, but it has been prepared directly as a Presentation on the above described subject. The Explanatory Notes are not the written version of the Presentation, but concepts, formulas and references that help with understanding the slides and preparing an eventual speaker to comment on them to an audience.

In detail, their scope is to enable the user who reads them to follow the Presentation easily and to get the greatest benefit from it. The user who, instead, chooses to carefully *study* them, would be able herself/himself to deliver the Review Talk. For this reason, there is some additional material in the Notes (arguments, references, formulas) for the benefit of a prospective speaker or any user who wants to deepen the knowledge on the subject.

The presentation runs also two movies in prefixed slides. These movies are especially devised for the Presentation and concern the Cosmological Simulations and The Universal Rotation Curve of galaxies.

It may be obvious, however, it could still be worth to stress that the Explanatory Notes without the .ppt Presentation are worthless. On the other hand, the Presentation Review file without the Notes is difficult to "use".

An other clarification maybe necessary: we are envisaging this Review as being one section of a virtual course on "Physical Cosmology" organized as follows: Big Bang Cosmology (3 x 45'), Structure formation (4 x 45'), Dark Ages and objects at high redshifts (3 x 45'), The distribution of DM in Groups, Clusters and larger scales (2 x 45'), The distribution of DM in Galaxies (2 x 45'), The physics of baryons in forming the luminous structure of Universe (4 x 45'), Candidates for the DM particle and their detection (3 x 45'), Alternatives to Dark Matter (1 x 45'). We have not written out this programme to anticipate a future project, but to frame this Review Talk in its Cosmological Context. More specifically, our Review aims to bring the user up to a good level of knowledge of its core subject: the Dark and Luminous matter distribution in galaxies. For other topics, which are occasionally touched on by the review, the user is redirected to more specialized reviews, lecture notes and books. And, of course, a number of issues involving DM will not be dealt in this Review.

Let us also stress that, contrary to the situation for written reviews, with this one it is up to the users, and not only the authors, to establish the relative and absolute importance of each statement, formula, reference and plot in the Presentation and eventually convey this to others.

1.2 Who may this Presentation Review + EN be useful to?

In order to avoid disappointments, it is worth to stress that this Review is neither designed as a public outreach talk on Dark Matter, nor as a Seminar that advertises a hot topic in Cosmology.

The target of this Presentation Review is the "Community" of thousands of physicists and astrophysicists whose work already touches, in many different ways, the subject of dark matter in galaxies and that would like to become more aware of the phenomenology behind this subject, possibly relevant for their research.

The success of DMAW 2010 has shown that this community is wide and that our dedicated efforts are well received. We hope that many people will be interested in downloading this Presentation + the Explanatory notes:

i) People who would like to follow this innovative approach so as to learn more about this increasingly important subject in Cosmology, Extragalactic Astrophysics and Astroparticle Physics, which they may often meet with in their own research work.

ii) PhD Students in any field of Astrophysics and Astroparticles

iii) Newcomers in Cosmology from different research fields.

iv) People who would like to deliver a well-tested Presentation Review to colleagues or students, for the reasons given above.

v) People that would like to have a reliable Review Presentation on an important subject that may be of help in the preparation of talks or lectures, centred either on this or on other adjacent topics.

1.3 Downloading

The Presentation Review, the Explanatory Notes, the two movies that run inside the Presentation and the Comments received for the DMAW 2010 Initiative can be downloaded at:

http://www.sissa.it/ap/dmg/dmaw_presentation.html

In detail, the names of the files of the downloadable material are:

The Presentation Review Talk "Dark Matter in Galaxies": DMGAL2010.pptx

Explanatory Notes: EXPLANOTES.pdf

Movies in the Presentation: movie1.mp4, movie2.wmv

The DMAW2010 Speakers' Reports and Comments: Comments.pdf

1.4 How to use this Presentation Review + EN ?

The following may be obvious but, to avoid misunderstandings, must be stressed for a correct and successful use of this material. The use of this innovative product requires significantly more time and personal effort than reading a Review Paper published in a Journal or in a Conference Proceedings Book. Users with profile (i-iii) above will need to invest and work a couple of half- days to read the Notes and to play the Presentation. For users with profile (iv) the requested effort is obviously greater. For users with profile (v), instead, the material we provide can save their working time and enable them to get improved results with less effort. Finally, let us talk about the users², that is, those who will be in the audiences of the users with profile (iv). They are the best off: with 90 minutes of attention they will get a good knowledge of the field, as it was the case for the audiences of DMAW 2010.

1.5 How to refer to/cite this Presentation Review + EN ?

Differently from the usual situation for reviews published in Journals and Books, the present new scientific product should not be cited in papers as the *unique* support reference for a result or for a view, also if they are its core subject. We believe that the credit to the results that this review wants to diffuse should go to the original papers. On the other hand, we would much like to ask people to advertise this Presentation Review as much as possible in papers and in other occasions (e.g. Social Networks etc), in terms of the aims described in Section 1.2

1.6 Comments and criticisms

They are welcomed, especially if they consist in modifications and additions in a form that, in case, allow us easily to take them into account.

1.7 Acknowledgments

We warmly and sincerely thank our colleagues, all the speakers, the LOC and the SOC because, without their willingness, suggestions and support, this product so as the whole DMAW 2010 initiative would not have been realized.

cfriгерio@ufabc.edu.br; Andrea.Lapi@roma2.infn.it, salucci@sissa.it

2 The Review Talk: Dark Matter in Galaxies

Abstract

This Review Talk concerns, in a detailed way, the mass discrepancy phenomenon detected in galaxies that usually we account by postulating the presence of a non luminous non baryonic component. In the theoretical framework of Newtonian Gravity and Dark Matter Halos, we start by recalling the properties of the latter, as emerging from the state-of-the-art of the numerical simulations performed in the current Λ CDM scenario of cosmological structure formation and evolution. We then report the simple, but much-telling, phenomenology of the distribution of dark and luminous matter in Spirals, Ellipticals, and dwarf Spheroidals. It will be shown that a coherent observational framework emerges from reliable data of different large samples of objects. The findings come after applying different methods of investigation to different tracers of the gravitational field. They include RCs and dispersion velocities profiles fitting, X-ray emitting gas properties analysis, weak and strong lens signal mass decompositions, analysis of halo and baryonic mass functions. We will then highlight the impressive evidence that the distribution of dark and luminous matter are closely correlated and that have universal characteristics. Hints on how this phenomenological scenario of the mass distribution in galaxies, including the Milky Way and the nearby ones, has a cosmological role, are given. Finally, we discuss the constraints on the elusive nature of the dark matter particle that observations pose to its direct and indirect searches.

3 Explanatory Notes for the Slides

Introduction

Slide 2

Dark Matter is a main actor in Cosmology. It rules the processes of formation and evolution of all the structures of the Universe, of which today it constitutes the great majority of the mass and an important fraction of the mass energy. Furthermore, it is likely made of an elementary particle, beyond the Standard Model, but yet not detected. However, this review will focus on just one specific aspect of this mysterious component, although a very crucial one: its distribution in galaxies, examined also in relation with that of the ordinary matter. The phenomenological scenario discussed in this Review Seminar can result a precious and unique way to understand how dark halos and their galaxies formed and what they are really made of and maybe approach ourselves to new laws or processes of Nature.

Slides 4

Galaxies, i.e. Spirals, Ellipticals, and Dwarfs spheroidals, have very likely just one type of dark halo. Their luminous components, instead, show a striking variety in morphology and in the values of their structural physical quantities.

The range in magnitudes and central surface densities is 15 mag and 16 mag/arcsec².

The distribution of the luminous matter is given by a stellar disk + a spheroidal central bulge and an extended HI disk in spirals and by a stellar spheroid in ellipticals and dSphs.

Slide 5

The best physical way to introduce the “phenomenon” of Dark Matter is the following: let us define $M(r)$ the mass distribution of the gravitating matter and $M_L(r)$ that of all baryonic components. We can obtain both distributions from observations; we first realize that, as we start moving from a certain radius r_T , function of galaxy luminosity and Hubble Type, outwards, these distributions increasingly do not match, $d \log M / d \log r > d \log M_L / d \log r$.

We are then forced to introduce a non luminous component whose mass profile $M_H(r)$ accounts for the disagreement:

$$\frac{d \log M(r)}{d \log r} = \frac{M_L(r)}{M(r)} \frac{d \log M_L}{d \log r} + \frac{M_H(r)}{M(r)} \frac{d \log M_H}{d \log r}.$$

This immediately shows that the phenomenon of the mass discrepancy in galaxies emerges from the discordant value of the radial derivative of the mass distribution, more precisely, from that of the circular velocity or that of the dispersion velocity, two quantities that measure it: $M \propto r V^2(r) \propto \sigma^2(r)$.

The DM phenomenon can be investigated only if we know well the distribution of luminous matter and we can accurately measure the distribution of the gravitating matter.

Slides 6

We briefly present the aspects related to the current theory of galaxy formation that are mostly relevant for this core topic of this Review.

Slides 7-8

It is worthwhile to briefly recall the predictions for the structure of DM halos coming from Λ CDM, the current theory of cosmological structure formation which is in well agreement with a number of

cosmological observations.

A fundamental prediction, emerging from N-body simulations performed in this scenario is that virialized dark matter halos have a universal spherically averaged density profile, $\rho_H(r) = \rho_{CDM}(r)$ (Navarro, Frenk, & White, 1997):

$$\rho_{CDM}(r) = \frac{\rho_s}{(r/r_s)(1+r/r_s)^2},$$

where ρ_s and r_s are strongly correlated (Wechsler et al., 2002, 2006), $r_s \simeq 8.8 \left(\frac{M_{vir}}{10^{11}M_\odot}\right)^{0.46}$ kpc. The concentration parameter $c \equiv r_s/R_{vir}$ is found to be a weak function of mass (Klypin et al., 2010) but a crucial quantity in determining the density shape at intermediate radii.

Notice that for any halo mass distribution $M_H(r)$: $M_{vir} \equiv M_H(R_{vir})$

The recent Aquarius simulation, the highest resolution to date, renders a single dark matter halo using 4.4 billion particles, of which 1.1 billion within the virial radius. We show spherically averaged density (left) and circular velocity (right) profiles. Curves with different colours correspond to different resolution runs, and the corresponding resolution limits are highlighted with arrows. These show that the spherically-averaged density profiles of Λ CDM haloes deviate slightly but systematically from the form found by NFW by using a much lesser number of particles and become progressively shallower inwards. However, these resolution differences are quite irrelevant and the NFW circular velocity well represent Λ CDM halos. Notice that the latter is almost never flat.

In any case, the actual profile is of very uncertain origin: departures from NFW shape are also seen in the halo velocity dispersion profile σ and the pseudo phase-space density emerges as a power law of radius: $\rho/\sigma^3 \propto r^{1.8}$ e.g. (Lapi & Cavaliere, 2009)

Slide 9

The movie shows the formation of one of the Aquarius halos, over nearly the full age of the Universe. The camera position moves slowly around the forming galactic halo, pointing towards its centre at all times.

4 Dark Matter in Spirals

Slide 11

The stars are distributed in a thin disk with surface luminosity (Freeman, 1970):

$$I(R) = I_0 e^{-R/R_D} = \frac{M_D}{2\pi R_D^2} e^{-R/R_D}$$

where R_D is the disk length scale, I_0 is the central value and M_D is the disk mass. The light profile does not depend on galaxy luminosity and the disk length-scale R_D sets a consistent reference scale in all objects and the extent of the distribution of the luminous component, we take $R_{opt} = 3.2R_D$ as the stellar disk size.

Although the mass modeling of some individual object and certain investigations require to accurately deal with the occasional presence of non exponential stellar disks and/or with the quite common presence of a central bulge, the above equation well represents, for the aim of this talk, the typical distribution of stars in spirals

Slide 12

Spirals have a (HI + He) gaseous disk with a (very) slowly decreasing surface density. This disk, at outer radii $R > R_{opt}$, especially in the case of low luminosity objects, is the major baryonic component and therefore must be carefully considered in the mass modeling. An inner H₂ disk is also present but it is negligible with respect to the stellar one (Wong & Blitz, 2002)

Slide 13

The kinematics in spirals (and more rarely in other objects) is measured by the Doppler Shift of well-known emission lines of particular tracers of the gravitational potential: HI, CO and H_α .

RadioTelescopes measure the galaxy kinematics by exploiting the 21 *cm* emission line. Notice the importance of the spatial resolution: since if we want to map a galaxy with a sufficient number of independent data also in the inner regions, the HI emission disk size must be at least 15-20 times bigger than the radiotelescope resolution beam, i.e. $\sim 200''$. There are relatively few objects in the Universe complying with this requirement.

WSRT (Westerbork Synthesis Radio Telescope) has a resolution of $12''$, VLA (Very Large Array) of $5'' - 15''$, ATCA (Australia Telescope Compact Array) of $15''$. The IRAM interferometer at Plateau de Bure measures CO RCs by means of the CO(1-0) transition at 2.6 mm, at a spatial resolution of $3''$.

Slide 14

Gran Telescopio Canarias is a 10.4 m diameter reflecting telescope at the Roque de los Muchachos Observatory on the island of La Palma.

In the summit of Hawaii dormant Mauna Kea volcano there are the twin Keck telescopes, the optical and the infrared. The telescopes primary mirrors are 10 meters in diameter and are each composed of 36 hexagonal segments that work in concert as a single piece of reflective glass.

The Large Binocular Telescope is located on 3,300 m Mount Graham in Arizona. The LBT is one of the world's highest resolution and most technologically advanced optical telescopes; the combined aperture of its two mirrors makes it the largest optical telescope in the world.

On Paranal ESO operates the ESO Very Large Telescope (VLT) with four 8.2-m telescopes. Each of them provides one Cassegrain and two Nasmyth focus stations for facility instruments.

In measuring optical RCs, the class of the telescope is not always decisive, but of course important. Telescopes in the 3-4 meter class are sufficient to provide high-quality optical kinematics for local objects. The biggest telescopes are necessary to measure the RCs at high redshifts.

Instead, in measuring dispersion velocities, new science usually requires the best telescopes, also for local objects.

Slides 15-16

We measure recessional velocities by Doppler shift, and from these, the rotation of the disk. In the process, we obtain the sky coordinates of the galaxy kinematical center, its systemic velocity, the degree of symmetry, the inclination angle and the circular velocity $V(R)$. Optical high quality kinematics can obtain circular velocity at a resolution $< R_D/10$.

Slides 17

During the 70's there was running the idea of a discrepancy between kinematics and photometry, already hinted in Freeman (1970) remarks about the NGC 300 RC. A topical moment was when Rubin published 20 optical RCs extended to R_{opt} that were still rising or flattish at the last measured point (Rubin et al., 1980). As a guide, we show the profiles of the stellar disk contribution if this was the sole contribution to the circular velocity.

Let us notice, however, that the actual contribution due to the stars, in view of the presence of a central bulge and, in some case, of a not exponential disk, may be inside R_{opt} flatter than how it has been drawn (but never rising).

4.1 Slide 18

The decisive measures that detected a dark component around spirals without doubt were obtained from the 21-cm RCs. Notice that HI line require radio telescopes with adequate sensitivity to detect the weak signals, and sufficient angular resolution to resolve the details. Only in the course of several decades the equipment improved, to arrive in the late 70' at conclusive results. A further improvement occurred later by using interferometers, based on combining the signals of two or more telescopes, and, by making use of the principle of earth rotation synthesis. Today maps of the integrated HI distribution and the radial velocity field are at a resolution of $< 10''$.

Bosma (1978, 1981a,b) collected data and compiled HI RCs for 25 galaxies well extended beyond the optical radius R_{opt} , indicated by a red bar on each curve. One obvious case is NGC 5055 shown in the slide. It is immediate that the RCs do not decline in a Keplerian way $\propto R^{-1/2}$ beyond this radius.

More quantitatively Bosma & van der Kruit (1979) obtained the surface photometry for these objects and found, in their outer parts, a clear increase with radius of the *local* mass-to-light ratios $\frac{dM/dR}{dL/dR}$. If light traces the gravitating mass, this quantity is expected to be constant with radius, equal to the average mass -to- light ratio of the stellar disk.

Slide 19

The radial Tully-Fisher relationship gives a most straightforward evidence for dark matter in spirals. The original paper of the standard TF relation is: Tully & Fisher (1977).

At different galactocentric distances, measured in units of the optical size, $R_i \equiv i R_{opt}$ ($i = 0.2, \dots, 1$), it has been observed the existence of a family of independent Tully-Fisher-like relationships, $M_{band} = b_i + a_i \log V(R_i)$ with M_{band} , the magnitude in a specific band, in detail the (R, I) bands.

This ensemble of relations, we call the Radial Tully-Fisher (Yegorova & Salucci, 2007), constraints the mass distribution in these objects. It shows a large systematic variation of the slopes a_i with R_i : they range across the disk between -4 and -8 . Moreover the RTF has a very small r.m.s. scatter at any radius. This variation, coupled with the smallness of the scatter, rules out the case in which the light follows the gravitating mass, shown in the figure as the black line predicting: $M_I = const_i + 10 \log V(R_i)$ for the case of a constant stellar mass-to- light ratio. However, also in the case of a magnitude dependence of the latter quantity, the slopes of the RTF could be different from the value of 10, but they should be all equal, at every R_i .

The RTF rules out mass models with no DM or with the same dark-to-luminous-mass fraction within $i R_{opt}$ in any galaxy.

Slides 20-21

Looking to individual RCs (right) we realize that their profiles are a function of the galaxy magnitude, a feature that points towards an universality of the spiral kinematics. Persic, Salucci, & Stel (1996) built 9 coadded RCs from about 700 individual RCs. The whole *I*-band luminosity $-16.3 < M_I < -23.4$ of spirals was divided in 9 luminosity intervals, each of them with ~ 1500 velocity measurements. For each interval the corresponding data were coadded in radial bins of size $0.3 R_D$ to build the synthetic curves $V_{rot}(R/R_{opt}, M_I)$ out to $\sim 1.2 R_{opt}$, $R_{opt} = 3.2 R_D$.

The coadded RCs result free from observational errors and non-axisymmetric disturbances present in individual RCs see Fig 1 and B1 of Persic, Salucci, & Stel (1996) and show a very small r.m.s. This result was confirmed by a similar analysis performed with 3000 RCs by Catinella, Giovanelli, & Haynes (2006) (points in the plot).

Slides 22

The URC is built from observations out to $6 R_D$. There are not reliable kinematical tracers outside this radius. It is possible, however, to extrapolate it out to virial radius (see Salucci et al. (2007)), the

bonafide radius of DM halos, (related to the virial mass by $R_{vir} = 260(M_{vir}/(10^{12}M_{\odot}))^{1/3}$ kpc) by using the galaxy virial mass M_{vir} and the virial velocity $V_{vir}^2 = G M_{vir}/R_{vir}$. The former can be obtained by weak lensing method (Mandelbaum et al., 2006, 2009) (left plot in the slide), and by correlating the galaxy baryonic mass function dN/dM_{bar} with the theoretical DM halo mass function dN/dM_{vir} (right plot). Two different recent works that have applied this method well agree with themselves and with weak lensing result. (Shankar et al., 2006; Vale & Ostriker, 2004; Marinoni & Hudson, 2002; Moster et al., 2010; Conroy et al., 2006). Then, at least in first approximation:

$$M_D = 2.3 \times 10^{10} \frac{(M_{vir}/M_s)^{3.1}}{(1 + (M_{vir}/M_s)^{2.2})} M_{\odot}$$

with $M_s = 3 \times 10^{11}$ that gives V_{vir} in terms of M_D , derived by the (known) inner URC.

Slides 23

These results lead to the concept of the Universal Rotation Curve (URC) of spirals. Let us define $x \equiv R/R_D$ and L the galaxy luminosity. We find that, for any x and L , the Cosmic Variance of $V(x, L)$, i.e. the variance of the circular velocity at a same radius x in galaxies of same luminosity L , is negligible compared to the large differences of $V(x, L)$ i) in a galaxy of luminosity L when x varies and ii) at the same radius x when L varies.

Therefore, the circular velocity at a given radius, this radius and the galaxy luminosity, lie on a smooth surface.

The URC is shown in the provided movie2 that should be linked to this slide.

Slides 24

The individual circular velocities $V(r)$, so as the coadded curves are the equilibrium circular velocities implied by the galaxy mass distributions. This allow us to decompose them in different mass components contributions. In detail, the gravitational potentials of a spherical stellar bulge, a DM halo, a stellar disk, a gaseous disk $\phi_{tot} = \phi_b + \phi_H + \phi_{disk} + \phi_{HI}$ lead to:

$$V_{tot}^2(r) = r \frac{d}{dr} \phi_{tot} = V_b^2 + V_H^2 + V_{disk}^2 + V_{HI}^2,$$

with the Poisson equation relating the surface (spatial) densities to the corresponding gravitational potentials. In general, we can neglect the contribution of the bulge, but this can play a crucial role in certain cases. HI surface density yields V_{gas}^2 , usually computed numerically. The contribution from the stellar exponential disk is

$$V_{disk}^2(r) = \frac{GM_D}{2R_D} x^2 B\left(\frac{x}{2}\right),$$

where $x \equiv r/R_D$, G and $B = I_0 K_0 - I_1 K_1$, a combination of Bessel functions.

For the DM component we follow the approach of (a quite general) Burkert empirical profile (Burkert, 1995)

$$\rho(r) = \frac{\rho_0 r_0^3}{(r + r_0)(r^2 + r_0^2)}$$

r_0 is the core radius and ρ_0 the central density. $V_{halo}^2 = GM_H/r$, $M_H = \int_0^R 4\pi r^2 \rho(r) dr$.

It is sometime used the pseudo-isothermal density $\rho(r) = \rho_0 \frac{r_0^2}{(r^2 + r_0^2)}$. We warn about this often used cored distribution (outside the baryonic regions of galaxies where any cored distribution is equivalent). In fact, it implies a divergent halo mass and a *outer* density profile inconsistent with that of NFW, in disagreement with observations.

Finally, we can adopt the NFW profile emerging out of N-body simulations.

The differences among the different halo profiles are shown in the plot.

The mass model has three free parameters: the disk mass, and two quantities related to the DM (the halo central density and core radius for Burkert halos). These are obtained by best fitting the data.

Notice that also for different Hubble type ellipticals, dSphs and for different techniques (weak lensing, dynamical modelling of dispersion velocity) the mass modelling always reduces in fitting the total gravitating mass profile $M(r)$ by means of a mass model that includes two components: $M_L(P_1, r)$ and $M_H(P_1, P_2, r)$ and it has, usually, three free parameters P_i (the mass in stars, the halo mass, the halo length scale).

Slides 25

We start by mass modelling the URC.

A Burkert halo + Freeman disk perfectly reproduce the coadded RCs at any luminosity. The luminous regions $R < 2R_D$ of the lowest luminosity objects are dark matter dominated, while in those of high luminosity objects, the stellar disk is the main mass component.

In any object, the dark component increases monotonically its importance on the circular velocity as R increases.

Importantly, the structural DM and LM parameters are related among themselves and with luminosity. In the 3D figure we see that spiral galaxies in the 4D space defined by central DM density, core radius, luminosity, fraction of DM at R_{opt} lie on a curve. On a physical side, we realize that smaller galaxies are denser and have a higher proportion of dark matter.

Slides 26-27

The relationships between halo structural quantities and luminosity must be investigated also via mass modelling of individual galaxies (Kormendy & Freeman, 2004) that sometime is helped by assuming that the stars dominate the very innermost regions. The results confirm the picture derived from the URC and point to the quantity $\rho_0 r_0$ which turns out to be constant in galaxies. Cored halos seem indispensable and smaller objects have always more proportion of dark matter.

Slides 28-29

The investigation of the density distribution of DM around spirals to check whether it complies with the ‘raw’ Λ CDM predictions needs careful model independent analysis of individual RCs.

This has been done by using suitable objects (Gentile et al., 2005), and also large galaxy samples, including the recent The HI Nearby Galaxy Survey of uniform and high quality data, with a significant number of rotation curves in which non-circular motions are small.

The available rotation curves are successfully fitted by a cored-halo + the stellar/HI disks. For DDO 47 the separate contributions are indicated. Instead, they are badly fitted by the NFW (or similar) halos + stellar/HI disks model, of which for IC 2575 we plot the separate components. The blue region indicates the discrepancy between NFW + disks models and actual data.

The results in these galaxies are quite typical. In addition to poor RC fits the latter mass model often leads to very large virial halo masses, and stellar mass-to-light ratio that result too low for the observed luminosities and colors of the galaxies. It is also proved that tri-axiality and non-circular motions cannot explain such CDM/NFW cusp discrepancy with the observed RC data of spirals and LSBs (Gentile et al., 2004; de Blok et al., 2008; Kuzio de Naray et al., 2008; Oh et al., 2008; Spano et al., 2008; Trachternach et al., 2008; Donato et al., 2009).

It is however worth recalling that several physical processes that modify the original cosmological NFW halo profiles to meet with the observed ones have been proposed. This discussion is beyond the aims of this talk, especially because consensus is far from being reached about the net effect of (baryonic) physical processes on the dark matter distribution: some physical processes make it close

to the observed (cored) (Governato et al., 2010), while others make the NFW cusp even steeper, e.g. (Gnedin et al., 2004).

5 Dark matter in ellipticals

Slide 32

In Ellipticals the surface brightness of stellar spheroid, the main baryonic component, follows a Sérsic (de Vaucouleurs) law:

$$I(R) = I_0 \operatorname{dex}[-b_n(R/R_e)^{1/n} - 1]$$

where n is the index of Sérsic defining the degree of concentration of the light and R_e is the half light radius. For $n = 4$ we obtain the well-known de Vaucouleurs profile. By deprojecting the surface density $I(R)$ we obtain the luminosity density $j(r)$ and by assuming a radially constant stellar mass to light ratio $(M/L)_*$, the spheroid density $\rho_{sph}(r)$. The central surface brightness μ_0 is given by: $\mu_0 = 2.5 \log I_0 + \text{const.}$

Slide 33

To derive the gravitational potential in Ellipticals and from this to infer the dark matter distribution is significantly more complicated than in spirals. The former can be obtained, always caveat a number of crucial assumptions, from dispersion velocities of stars or planetary Nebulae, from the X-ray properties of the emitting hot gas halos that lies around them, or from a combination of weak and strong lensing data.

Jeans equation is a crucial link between observations and data. We infer from the observed motions the underlying gravitational potential. The knowledge of the distribution of dark and luminous matter in these systems of different morphology, age and formation process, is however indispensable.

Slides 34

In ellipticals the kinematics is complex, the stars are in gravitational equilibrium by balancing the gravitational potential they are subject to with 3D motions, whose r.m.s exerts a pressure. Obviously, from the motions of stars in a galaxy we cannot measure the radial/tangential velocity dispersions, directly linked to the mass profile, but recessional velocities or projected and aperture velocity dispersions, quantities that are a much more indirect tracer of the gravitational potential, as shown by the formula in the slide, valid for case of isotropic orbits. The kinematics and its analysis becomes more complicated when this assumption is relaxed and/or some rotation is present.

In this case the full 2D kinematics is absolutely required and we must solve (with some assumption) the anisotropic Jeans equation, i.e. that involves also the higher moments of the LVDS at any position in the galaxy (Cappellari, 2008; Krajnović et al., 2005).

Slide 35

Ellipticals are quite compact objects, with respect to spirals. Stellar kinematics of the spheroid traces a very inner region of the DM halo, where likely it has small dynamical effect. Moreover, the analysis is far from straightforward. This can be seen when we try to reproduce the (observed) velocity dispersion profile $\sigma_{ap}(R)$ with a reasonable model made of a dark halo and a luminous mass component. We take a galaxy with a spheroid of $10^{11} M_\odot$ with the standard Sérsic parameter $n = 3$, a NFW halo with $c = 7$ and a mass 20 times bigger than that of the spheroid. In this mock object the DM has an important role, and it would emerge if its gravitational potential was probed by the rotation curve. However, when probed by σ_{ap} , the nature itself of this kinematical hides the dynamical effect of the

dark component (Mamon & Lokas, 2005). For a cored halo or with the presence of anisotropy the situation would be worse.

A similar result comes from the work of Tiret et al. (2010) in which it is shown that an assumed typical NFW DM halo around an elliptical, i.e. with $M_{vir} < 10^{14} M_{\odot}$, contributes to the observed central aperture velocity dispersion (e.g. to $\sigma_{ap}(1/2 R_e)$) in a negligible way: $\sigma_{ap,H}(1/2 R_e)^2 < (100 \text{ km/s})^2 \ll (\sigma_{ap})^2$. For cored halos the contribution is even smaller. Only the smallest ellipticals and dwarfs spheroidals in which $\sigma_{ap}(1/2 R_e) < 100 \text{ km/s}$, the stellar velocity dispersion may probe the dark component.

Slide 36

Important information on the mass distribution can be obtained from the Fundamental Plane. For virialized stable objects one expects the balance between the potential and kinetic energies.

$$\sigma^2 \propto \frac{GM_{dyn}}{R} \propto \frac{M_{dyn}}{L} \frac{L}{R^2} R \propto \frac{M_{dyn}}{L} I R,$$

where σ is a velocity dispersion, I is a surface luminosity, R is a scale, and M_{dyn}/L is the mass-to-light ratio. This implies a relationship between the observed velocity dispersion σ_e^2 , R_e and surface luminosity $I_e \equiv L_e/(2\pi R_e^2)$. i.e. a (Fundamental) Plane in the space of these 3 quantities. From the virial equilibrium, we expect: $R_e = \sigma_0^a / I_0^b$.

This relationship is found in ellipticals and S0: in the 3D space of $(R_e, \sigma_0, < I_e >)$, where the latter is the surface brightness inside R_e (Jorgensen et al., 1996) we have:

$$\log R_e = 1.24 \log \sigma_0 - 0.82 \log < I >_e$$

the scatter is very small, 0.07 dex in $\log R_e$

A similar results is found in the large sample of ellipticals that include 6000 objects of the digitalized survey SDSS (Hyde & Bernardi, 2009).

The very small scatter of objects around this plane suggests some degree of universality in their *inner* mass profile.

The value of the coefficient a is different from that expected by the virial theorem, $a = 2$ in the case in which ellipticals have the same dynamical mass-to-light ratio. This tilt of the FP can explained in a dependence of the stellar mass to light ratio (M_{sph}/L) on luminosity (spheroid mass). In fact, FP residuals are found correlated with stellar population characteristics as line- strength indices and are anticorrelated with the abundance ratio α/Fe , (Gargiulo et al., 2009).

Slide 37-39

Planetary Nebulae (PN) provide us with the elliptical galaxy kinematics out to many effective radii, (Méndez et al., 2009). The use of dedicated instruments, like the Planetary Nebula Spectrograph (Douglas et al., 2002) has strongly powered the technique, so that distances comparably to those reached by extended HI disks in spirals can be probed (Coccatto et al., 2009).

In each galaxy 200 individual PN radial velocity measurements are usually obtained. By binning PN radial velocities in elliptical bins, or in strips over the major and minor axes (see for details (Napolitano et al., 2001)), reliable 2D kinematical maps have been derived (Coccatto et al., 2008). These maps led to independent and high quality projected velocity dispersion measurements out to $(5 - 8)R_e$, with a typical spatial resolution of $1/3 R_e$.

A systematic study of the velocity dispersions in a dozen of objects has revealed that in the most luminous objects the velocity dispersion tends to show a regular, monotonic flat profile, that poses no problem in the subsequent mass modelling, other than its uniqueness (Coccatto et al., 2009; Napolitano et al., 2010).

In low luminosity objects, instead, the PNs velocity dispersion profile show a large pseudo-and ultra-keplerian decline: $\sigma_P \propto R^a$ with $a < -0.5$. To analyse these data obviously requires a full

modelling of a very likely complex dynamics, that includes also an appropriate treatment of the orbital anisotropies of the tracers.

For objects with “regular” kinematics the best case analysed so far is NGC 4374 (Napolitano et al., 2010) where a flat dispersion profile has been derived from about 450 PNes and then modeled by means of Jeans analysis.

As result, a variety of halo model profiles including NFW, some of its variants and the cored URC halo, in cooperation with a spheroid with typical mass-to-light ratios, well fit the data, confirming the presence a very massive dark halo. Notice that in this elliptical the kinetical energy $\propto V_{rms}^2$ has both rotational and random motions component: $V_{rms} = (V_{rot}^2 + \sigma_P^2)^{1/2}$.

Slides 40-42

Gravity bends light and this can be used to weigh the galaxy mass, e.g. the pioneering work by (Schneider, 1996). We know that a background round galaxy (of semi axis $a/b = 1$) whose line of the sight passes at distance R_P from a the center of a galaxy put at a convenient distance (half way between us the background) will be seen with a (very small) ellipticity $a/b - 1 \simeq 10^{-3}$. The ellipticity of a galaxy image is an unbiased estimate of the local shear. When averaged on a very large number of source galaxies whose lines of sight all pass around a lens, we can meaningfully measure the tangential shear γ_t of the lens. The lens equation relates γ_t with the distribution of matter in the lensing galaxy:

$$\gamma_t = (\bar{\Sigma} - \Sigma(R))/\Sigma_c,$$

where $\Sigma(R) = 2 \int_0^\infty \rho(R, z) dz$ is the projected mass density of the object distorting the galaxy image, at projected radius R and $\bar{\Sigma}(R) = \frac{2}{R^2} \int_0^R x \Sigma(x) dx$ is the mean projected mass density interior to the radius R . $\Sigma_c \equiv \frac{c^2}{4\pi G} \frac{D_s}{D_l D_{ls}}$, where D_s and D_l are the distances from the observer to the source and lens, respectively, and D_{ls} is the source-lens distance. The above relations directly relate observed signals with the underlying DM halo density. A very detailed explanation of the weak lensing phenomenon can be found in the second chapter of Schneider, P., Kochanek, C. S., & Wambsganss, J. (2006).

Let us stress that we discuss this effect in the section of elliptical in that it has been applied mostly for these objects, however there are applications (even in this Review) for Spirals.

The DM distribution is obtained by fitting the observed shear with a chosen halo density profile with 2 free parameters. The method is clean because it is free from the baryonic contribution, but the signal is intrinsically weak. Mandelbaum et al. (2009, 2006) measured the shear around 1.7×10^5 isolated galaxies of different luminosities and Hubble Type, by using 3×10^7 SDSS galaxies as sources. The measurements extended out to 500 – 1000 kpc reaching out the virial radius of the lens galaxies. Although the structural DM parameters were determined with quite large uncertainties, the NFW and Burkert halo profiles, not much different at outer radii, both agree with the data. No relevant difference in the DM distribution around ellipticals or spirals emerged.

Very importantly, the virial halo masses so determined are found to correlate with the galaxy luminosities. When this relation is coupled with the well known mass vs. light relationship of the stellar component, it leads to the fact that the amount of baryons M_{bar} today in a galaxy is a function of M_{vir} , the mass of the halo surrounding the galaxy. We consider this as the main relationship of the galaxy formation process. It is interesting to note that $M_{vir}/M_{bar} \gg 7$, the cosmological value.

Noticeably, when we fit the tangential shear with a Burkert profile, we obtain the same values of halo structural parameters ρ_0 , r_0 derived by mass modelling the URC or individual galaxies (Donato et al., 2009).

Slide 43-44

Koopmans et al. (2006) performed a joint strong lensing + stellar-dynamical analysis of a sample of 15 massive early-type galaxies selected from the SLACS Survey. Given the smallness of the radial range investigated, the total mass density was assumed a power law without loss of generality. The

spheroid component, was represented for simplicity, as an Hernquist profile, very similar inside R_e to a Sérsic one. Velocity dispersions at R_e provided the additional constraint to the mass distribution, that was investigated through Jeans Equation.

They found, independently of the DM density profile in the region under investigation, that these massive early-type galaxies have remarkably the same inner *total* density profiles ($\rho_{tot} = \rho_H + \rho_{sph} \propto r^{-2}$). The figure shows the logarithmic density slope of SLACS lens galaxies as a function of (normalized) Einstein radius. Moreover, they found that the stellar spheroid accounts for most of the total mass inside R_e .

In both cases, given the smallness of the dark component inside R_e , the small radial range, the not negligible observational error and the relevance of the assumptions taken, it is not possible to constrain the actual profile of the dark halo.

Slide 45

Isolated Ellipticals have a X-ray emitting halo of regular morphology, that, extends out to very large radii, providing us with a reliable mass distribution. The gravitating mass inside a radius r , $M(r)$ can be derived from their X-ray flux by assuming that the emitting gas is in hydrostatic equilibrium. The observed X-ray surface brightness, gives, by means of the well known β -model, the gas density distribution. From the hot gas density and temperature profiles (Fabricant, Rybicki, & Gorenstein, 1984), we have:

$$M(< r) = \frac{kT_g(r)r}{G\mu m_p} \left(\frac{d \log n}{d \log r} + \frac{d \log T_g(r)}{d \log r} \right)$$

where T_g is the gas temperature at radius r , ρ_g is the gas density, k is the Boltzmann's constant, G is the gravitational constant, μ is the mean molecular weight $\mu = 0.62$ (Ettori & Fabian, 2006), and m_p is the mass of the proton.

Nagino & Matsushita (2009) analyzed a sample of 22 objects with XMM-Newton and Chandra data out to $10 R_e$. They confirmed the presence of DM in any object, but this component was found dynamically important only outside R_e , where the mass-to-light ratio is found to start to increase. Furthermore, there is some hint that, outside this radius, the halo mass increases with radii quite steeply suggesting a cored DM halo density, for which the dark mass increase rate between r^3 and r^2 .

Slide 46

The gravitating matter in form of stars M_* is a crucial quantity. It defines the efficiency of the process of forming this (luminous) component from the cosmological hydrogen. Usually, it is obtained as result of the kinematical mass modelling, but in some case its resulting value has a very large uncertainty. This, in turn complicate the full investigation on the Dark Matter distribution. Moreover, in low luminosity and DM dominated objects, the kinematics cannot provide a reliable estimate of the stellar disk mass.

It is well known that the galaxy luminosity is related to its stellar content. Hence the straightforward approach to obtain the stellar mass of a galaxy is to model its luminosity in terms of age, metallicity, initial mass function. This modelling is provided by Stellar Population Synthesis models. This method is presented in this section since it has important applications in Ellipticals, but it is applied also to Spirals and dSphs.

The observed Spectral Energy Distribution (SED) of a galaxy, or selected colour indices or absorption lines, is fitted with models calculated under different assumptions regarding the IMF, the star formation history, the metallicity, etc. The same modelling naturally provides the amount of stellar mass that is implied by the different fits (for a classical paper see Tinsley (1975)). In practice, degeneracies between age, metallicities and dust content make it sometimes hard to select the actual physical model for the galaxy light just in terms of fit goodness. Observations are decisive to solve these intrinsic uncertainties.

While the best approach is obviously to fit the whole spectral energy distribution, as this allows a better handle of elusive degeneracies, often not all observational bands are available for galaxies. A simplified approach was suggested by Bell & de Jong (2001) who noted that rather simple relationships exist between mass-to-light ratios in certain bands and some colour indices of population synthesis models (from various codes). These relations have been calibrated using spiral galaxies. In the plot there are two different M/L 's as a function of (B-R), for a sequence of exponentially declining star formation rate models of age 12 Gyr obtained by using a variety of Stellar Population Synthesis models. The red end of the lines represent a short burst of star formation, the blue end represents a constant star formation rate model. The different models used are: Bruzual & Charlot, Kodama & Arimoto, Schulz et al. and PEGASE by Fioc & Rocca-Volmerang all with a Salpeter Initial Mass Function.

Recent work considers in great depth the TP-AGB phase of stellar evolution while building the galaxy SED (Maraston, 1998, 2005) which were shown to provide a better fit to the spectral energy distribution of high-redshift galaxies (Maraston et al., 2006), allowing to better determine their stellar masses. The resulting mass-to-light ratios, as a function of galaxy color are shown in the slide.

Slide 47

The photometric estimates of stellar disk/spheroid masses are tested with respect to the kinematical estimate of the mass in stars.

In Salucci et al. (2007) the disk masses of 18 spiral galaxies of different luminosity and Hubble Type have been derived both by mass modelling their rotation curves and by fitting their SED with spectro-photometric models. The two estimates result in perfect proportionality and the agreement between the two different estimates is less than 0.15 dex.

In Elliptical galaxies the determination of dynamical mass inside R_e can be performed by assuming that a De Vaucoulers spheroid is the main component then: $M_{dyn} = 1.5 \times 10^{10} (\sigma_e/200 \text{ km/s})^2 (R_e/kpc) \dot{M}$. This dynamical estimate of the “stellar” mass is found to well correlate with the red luminosity, i.e. with a measure of the photometric mass estimate (Shankar & Bernardi, 2009).

Grillo et al. (2009) studied a sample of Ellipticals with Einstein rings and derived the total projected mass enclosed within them. Then, by using the SDSS multicolor photometry fitted the spectral energy distributions (SEDs) (ugriz magnitudes) with a three-parameter grid (age, star-formation timescale, and photometric mass) of Bruzual & Charlot's and Maraston's composite stellar-population models, and various initial mass functions (IMFs). The two different mass estimates agreed with 0.2 dex.

A similar result has been obtained by studying a sample of ellipticals with detailed axisymmetric dynamical modelling of 2D kinematics (Cappellari et al., 2006).

Caution: the disagreement among dynamical and spectro-photometric estimates is about 0.15 dex, this value is small for cosmological implications, i.e. to build a stellar mass function from a luminosity function, but it is extremely large for mass modelling. The induced error, if we assume $(M_*/L)^{SPS}$ in estimating the DM profile

$$\rho_H(r) = \frac{1}{4\pi r^2} d(M_{dyn}(r) - (M_*/L)^{SPS} L(r)) / dr$$

can totally err the derived density profile.

6 Dark matter in dwarf spheroidals

Slide 50

Dwarf spheroidal (dSph) galaxies are the smallest and least luminous galaxies in the Universe and so provide unique hints on the nature of DM and of the galaxy formation process. Early observations (e.g. Aaronson (1983)) of stellar kinematics in the brightest ($L_V \sim 10^{5-7} L_{V,\odot}$) of the Milky Way's dSph satellites found that they have central velocity dispersions of $\sim 10 \text{ km s}^{-1}$, larger than expected

for self-gravitating, equilibrium stellar populations with scale radii of ~ 100 pc. The recent discoveries of ultra-faint Milky Way satellites (e.g. Willman et al. (2005); Belokurov et al. (2007)) extend the range of dSph structural parameters by an order of magnitude in (luminous) scale radius and by three orders of magnitude in luminosity.

The distribution of total luminosity and of the central stellar velocity dispersion in star clusters and in dSphs overlap. The faintest galaxies have approximately the same values of these physical parameters of star clusters, with galaxy luminosity extending down to $10^3 L_\odot$. In dSphs the half-light radii, however, are significantly larger (hundreds of parsecs) than those of star clusters (tens of parsecs). This leads, through the virial theorem, to significantly larger masses in dSph.

The values of central and global mass-to-light ratios for the gas-poor, low-luminosity, low surface brightness satellites of the Milky Way are high, up to several hundred in solar units, making these systems the most dark matter dominated galaxies in the local Universe (Mateo, 1998).

Slide 51

DSphs are old and apparently in dynamical equilibrium, with no dynamically-significant gas. They contain a (small) number of stars, which provide us with collisionless tracer particles. Aaronson (1983) measured the velocity dispersion profile of Draco based on observations of three carbon stars, finding a mass-to-light ratio an order of magnitude greater than that found for galactic globulars. Mateo (1997) provided the first dispersion velocity profile of Fornax. With the new generation of wide-field multi-object spectrographs on 4-8m telescopes, it is now viable to obtain sufficient high-quality kinematic data to determine the gravitational potentials in all the Galactic satellites.

Slide 52

Walker et al. (2007) published high quality velocity dispersion profiles for seven Milky Way satellites. They are generally flat out to large radii, in terms of the half light radii that determine the sizes of the baryonic matter in these objects. These data indicate that almost all of their gravitating mass is unseen, i.e. in a DM halo.

Slide 53-54

The mass modelling of these object is not immediate, in that the distribution of the stars, that are the tracers of the gravitational fields, must be known with precision. Moreover, the relation between mass and dispersion velocity is not a straightforward one: in a collisionless equilibrium system that of the stellar spheroids in dSph, the Jeans equation relates the kinematics of the tracer stellar population and the underlying (stellar plus dark) mass distribution. Assuming spherical symmetry, the mass profile can be derived as

$$M(r) = -\frac{r^2}{G} \left(\frac{1}{\nu} \frac{d \nu \sigma_r^2}{dr} + 2 \frac{\beta \sigma_r^2}{r} \right),$$

where $\sigma_r(r)$, $\beta(r)$ and $\nu(r)$ are, respectively, the stellar velocity dispersion component radially toward the center of the mass distribution, the velocity anisotropy and the stellar density distribution.

Disadvantages in modeling these systems are: i) it is required to take some assumption on the velocity anisotropy and ii) derive the stellar density profile with precision, in order to fit the observed velocity dispersion profile and obtain a reliable DM distribution.

An advantage is that their luminosities are so small that we can always exclude that baryons play a (complicated) role in the mass modelling.

The surface brightness profiles are typically fit by a Plummer distribution (Plummer, 1915)

$$\nu(R) = \frac{\nu_0}{(1 + R^2/R_b^2)^2},$$

where R is the projected radius, ν_0 is the central surface density and R_b is stellar length-scale Notice that, if we want to derive the DM density profile (not its amount) we must know with good accuracy

the distribution of the stellar component, since this quantity enters in the determination of the mass *profile* in a non-linear way. In Elliptical and Spirals, it is instead extremely rare that, given a set of kinematical data, two different stellar distributions but both compatible with the measured surface photometry, yield, in the mass modelling, different DM profiles.

The analysis of the mass distributions obtained from isotropic Jeans equation analysis of six dSphs by Gilmore et al. (2007b) favor a cored dark matter density distribution.

However, ? applying the Jeans equation to eight brightest dSphs and relaxing the isotropy assumption found that the dispersion velocities of these objects can be fit by a wide range of different halo models and velocity anisotropies. In particular cusped and cored dark matter mass models can fit the dispersion profiles equally well.

Slide 55

A resolute fact could be that dSphs cored distribution structural parameters surprisingly agree with those of Spirals and Ellipticals: Donato et al. (2009) have shown that a Burkert halo density profile reproduces the dispersion velocity of six Milky Way dSphs and that the derived halo central densities and core radii are consistent with the extrapolation of the relationship between these quantities found in Spirals. This intriguing result, beside supporting cored distribution in dSph, could point to a common physical process responsible for the formation of cores in galactic halos of all sizes or to a strong coupling between the DM and luminous matter.

Slide 56

The dark+ stellar mass within the effective radii of dSph galaxies have been suspected for some years of showing a remarkably small range (Mateo, 1998). The available data seem to be consistent with an (apparent) minimum dark halo mass, supported also by the presence of a strong relationship between M_*/L_V and L (Wilkinson et al., 2006; Gilmore et al., 2007a).

More explicitly, a relationship is found for which, within 300 pc, all object seem to possess the same mass, of the order of $10^7 M_\odot$, (Côté et al., 1999; Strigari et al., 2008; Gilmore et al., 2007b). This relationship maybe be not intrinsic, but due to the universality of the profile of the density of the halos around galaxies.

On the other hand, if all dSphs are embedded within an "unique" dark matter halo, this could explain the finding that their masses increase as power-law in all objects, $M(r) \propto r^{1.4}$ (Walker et al., 2009).

Slide 58

DM halos around galaxies form a family of dark spheres with their virial mass being the order parameter. It is possible to work out an unified scheme for their structural characteristics, that, let us remind, are derived by means of several different methods in galaxies of different luminosities and morphologies. From all available data a picture emerges: DM halos around spirals, LSBs and dSphs and Ellipticals can be well represented by a Burkert profile with a core radius r_0 and a central density ρ_0 .

Very intriguingly: the halo central surface density $\propto \rho_0 r_0$ is found nearly constant and independent of galaxy luminosity. This result come from the mass models of 1) about 1000 coadded rotation curve of Spirals, 2) individual dwarf irregulars and spiral galaxies of late and early types 3) galaxy-galaxy weak lensing signals 4) kinematics of Local Group dwarf spheroidals.

It is found:

$$\log(r_0 \rho_0) = 2.15 \pm 0.2$$

in units of $\log(M_\odot/pc^2)$.

This results are obtained for galactic systems spanning over 14 magnitudes, belonging to different Hubble Types, and whose mass profiles have been determined by several independent methods. In the

same objects, the constancy of $\rho_0 r_0$ is in sharp contrast to the systematical variations, by 3-5 orders of magnitude, of galaxy properties, including ρ_0 and central *stellar* surface density.

Slide 59

A connection between the a-priori independent distributions of dark and luminous matter in galaxies emerges strongly. The velocity (mass) profile, despite being the sum in quadrature of *both* components, can surprisingly be fully represented by a function that includes only one of them. In fact, for Spirals, (but likely in galaxies of other Hubble Types) we have : $V(r) = F_{bar}(r/R_D, M_I)$ (M_I is the I- band magnitude, left- side plot), but, at the same time, we also have: $V(r) = F_{vir}(r/R_{vir}, M_{vir})$ (right-side plot) (Salucci et al., 2007).

In this last case the baryonic component breaks the mass invariance of the RC profile due to the DM component, but in a mass dependent way. The differences of the inner RCs profile of high and low mass objects are due to differences in the fractional content of baryonic matter, but mysteriously, they, in turn, depend on the halo mass.

It may be worth recalling that similar result (in qualitatively way) are present in the predictions of Λ CDM, where NFW halos coupled with a stellar disks formed according to the Mo et al. (1998) theory leads to RCs Universal profile, function of the halo virial mass.

Slide 60

Moster et al. (2010) used a statistical approach to determine the relationship between the stellar masses of galaxies and the masses of the dark matter halos in which they reside. They obtained (following Shankar et al. (2006)) a stellar-to-halo mass (SHM) relation by populating halos and sub-halos in an N-body simulation with galaxies and requiring that the observed stellar mass function be reproduced. The existence of this non linear relation is not trivial: M_* , the mass in stars, does not scale proportionally to M_{vir} and it is much smaller than that expected by the Cosmological value (blue line) $\Omega_{baryons}/\Omega_{DM}$.

Walker et al. (2010b), subtracted in spirals and in dSph the baryonic contributions to the overall gravitational potential to derive the contribution to rotation curves due to dark matter halos at intermediate radii. They found that, in physical units, these RCs are remarkably similar, with a mean curve given by

$$\log \frac{V_H}{(km/s)} = 1.47^{+0.15}_{-0.19} + 0.2 \log (r/kpc)$$

Evaluation at specific radii of this Universal Profile immediately generates two results discussed above: a common mass for MW dSphs at fixed radius and a constant DM central surface density for galaxies ranging from MW dSphs to spirals. This result is very remarkable: in the Universal Functions discussed above as the URC and the FP, the radial unit is always measured in terms of the stellar galaxy size and not, as here, in physical units.

However, in dSphs it is possible to estimate “the circular velocity” only at one radius in each galaxy (Walker et al., 2009), namely the half light radius, whose definition itself, however, may be not trivial (Walker et al., 2010a).

This very recent result needs more investigation, though it seems coherent with the phenomenology of the DM distribution around galaxies.

Slide 61

Let us define R_e as the effective radius encompassing *half* of the mass of stellar component and provides so a the measure of the size of the latter. At R_e in dispersion-supported galaxies, within a large range of luminosities, the dynamical mass-to-light (M/L) ratios can be obtained (Wolf et al., 2010). At the

high mass end, these estimates come from the FP, while at the low mass end, they come from Jeans modelling of dwarf spheroidal galaxies.

Confronting the emerging mass-to-light ratios, galaxies follow a characteristic U-shaped curve (Wolf et al., 2010), where M/L is minimized for $\sim L^*$ galaxies and rises at both low and high masses. This can be seen in the plot, where the I -band M/L ratio within the half-light radius is plotted against the mass contained within the half-light radius.

One can interpret this as the inverse efficiency with which galaxies retain and turn their initial quotient of baryons into stars : $1/7 M_{vir}$. There must be two mechanisms that prevent galaxies from turning their initial baryons into stars, one of which operates most efficiently at low masses, switching on strongly below $M(R_e) < 10^8 M_\odot$, and one of which operates most efficiently at high mass, gradually becoming more effective at masses above $M(R_e) > 10^{11} M_\odot$. Some suggested mechanisms for the former include heating from re-ionization, supernova feedback, and tidal and ram pressure stripping for those galaxies that are satellites, while proposals for the latter mechanism are feedback from active galactic nuclei, virial heating of gas in the deep potential well, and supernova feedback.

It is interesting that, globular clusters, whose masses can be calculated using the same Jeans modelling methods as those of dwarf spheroidal galaxies, are unambiguously not part of this relation. They have roughly constant M/L ratios, consistent with that expected from their stellar populations. Systems containing dark matter and those without dark matter are therefore easily distinguished.

It is worth recalling that the same U shape is seen in *disk systems* at R_{vir} (Shankar et al., 2006) and it is shown as yellow region in the plot.

7 Dark matter searches

Slide 62

To introduce the various candidates proposed as the Dark Particle and to discuss the present status of their possible detection would need a complete (long) Presentation Review. As matter of fact we deal these subjects in a brief section of our Review. This is certainly insufficient however this Presentation is likely to be for some the first (serious) contact with the DM world, and therefore we must consider here such issue.

Slides 63-65

DM is actively searched in a direct and indirect way. The distribution of dark matter in our galaxy, so as in nearby ones, plays an important role in it.

Among the many candidates suggested for dark matter but as yet undetected, one among the most compelling possibility is that the dark matter is comprised of Weakly Interacting Massive Particles, or WIMPs, a general class of particles, thermally produced in the hot early universe, which drop out of equilibrium when they are not relativistic. Bertone et al. (2005) discuss the theoretical motivations and introduce a wide array of candidates for particle dark matter.

Its density today is inversely proportional to their annihilation rate, and in order to represent the “CMB observed” $\sim 25\%$ of the critical density of the Universe, the particle’s annihilation cross section should be typical of electroweak-scale interactions, hinting at physics beyond the Standard Model. The existence of such a particle has plenty of theoretical justification. In fact, several extensions to the Standard Model lead to WIMP candidates. One of them is Supersymmetry (SUSY), which extends the Standard Model to include a new set of particles and interactions that solves the gauge hierarchy problem, leads to a unification of the coupling constants, and it is required by string theory. The lightest neutral SUSY particle, the neutralino, is thought to be stable and is a natural dark matter candidate.

Direct detection of WIMPs requires sensing scattering between WIMPs in the halo and atomic nuclei in a terrestrial detector. Despite the expected weak-scale coupling strength for such interactions, terrestrial experiments are made feasible by the fact that: i) the local DM mass-energy density is 10^5

times higher than that of the universal average. In detail, let us stress that $\rho_H(R_\odot)$, the DM density at the Sun location, has been recently estimated in an independent way by Salucci et al. (2010): $\rho_{DM}(R_\odot) = (0.43 \pm 0.1) \text{ GeV cm}^{-3}$ a value somewhat larger than that of 0.3 GeV cm^{-3} usually assumed. ii) coherence effects may amplify the interaction rate (e.g. spin-independent nuclear elastic scattering is proportional to A^2 the atomic weight of the target).

Even though direct detection may be possible, it is by no means easy. The energy of the resulting nuclear recoils is likely of order 20 keV, where electromagnetic backgrounds dominate by many orders of magnitude. Nuclear collisions due to neutrons also pose a serious obstacle, as they may exactly mimic those due to WIMPs. Hence, the fundamental challenge of a direct search is to identify extremely rare DM-induced nuclear recoil events from a vast array of spurious signals. This can be achieved by combining low-radioactivity materials and environments with robust background rejection of electron recoil events. These detectors must also be situated in deep underground laboratories to shield from cosmic-ray-induced backgrounds.

The dark matter community has developed a broad range of techniques to address these challenges. Many different experiments are currently pursuing one or more of the multiple possible detection channels. The most common technique is to look for ionization and/or scintillation of the detector medium (e.g. NaI, CsI, Ge, liquid/gaseous Xe or Ar) resulting from a WIMP-nucleon collision. Other experiments look for phonons, bubble nucleation, directionality effects.

About 50% of all direct search experiments use noble liquids (including XENON, LUX, XMASS, ZEPLIN, WARP, ArDM, and DEEP/CLEAN). Noble liquids, especially Xe and Ar, are promising as a detection medium as they are efficient scintillators, are chemically stable, and have relatively high stopping power due to high mass and density.

At present, the upper limit on the WIMP-nucleon cross section approaches 10^{-44} cm^2 , which is well into the region of parameter space where SUSY particles could account for the dark matter. The next 2-3 orders of magnitude represent a particularly rich region of electroweak-scale physics. The next generation of direct search experiments are poised to verify or reject a large portion of the current theoretical explanations of WIMP-like DM.

Slides 66-68

DM particles makes the galactic halo where they would continuously annihilate into quark or gauge boson pairs leading eventually to rare antimatter particles and high-energy photons and neutrinos. The indirect searches of DM are based on astrophysical observations of the products of DM self annihilation or decay. Given the known long lifetime of the DM, the signal for decay products is suppressed for heavy candidates (due to the combination of low number densities and long lifetime) leaving in most of the cases only the self-annihilation as most sensitive possible source of a signal. Antimatter particles such as antiprotons and positrons are interesting because they are quite rare in Nature. Any (additional) production through DM annihilation will induce an excess in the energy distributions of the flux observed at the earth. However, let us stress that conventional astrophysical mechanisms in the galaxy also produce antiprotons and positrons.

The indirect searches of DM are based on astrophysical observations of the products of DM self annihilation or decay. Given the known long lifetime of the DM, the signal for decay products is suppressed for heavy candidates (due to the combination of low number densities and long lifetime) leaving in most of the cases only the self-annihilation as most sensitive possible source of a signal.

In the case of searches via gamma ray observation, the expected flux in a detector on Earth is given by:

$$\frac{d\phi_\gamma}{dE_\gamma}(E_\gamma, \Delta\psi) = \frac{\langle\sigma v\rangle_{ann}}{4\pi m_\chi} \sum_f B_f \frac{dN_\gamma^f}{dE_\gamma} \times \frac{1}{2} \int_{\Delta\psi} \frac{d\Omega}{\Delta\psi} \int_{l.o.s.} dl(\psi) \rho^2(r), \quad (1)$$

where E_γ is the photon energy, m_χ is the DM particle mass, $\Delta\psi$ is the detector opening angle, $\langle\sigma v\rangle_{ann}$ is the mean annihilation cross section times the relative velocity (of order $10^{-26} \text{ cm}^3 \text{ s}^{-1}$ for cold WIMP relics from abundances constrains), B_f indicates the branching fraction in a given channel f , $\frac{dN_\gamma^f}{dE_\gamma}$ is

the photon spectrum for a given annihilation channel which depends on the DM model and can have both continuum and discrete lines contributions, ρ is the DM density and the integrals are along the line of sight and over the detector angle.

The quadratic dependence on ρ suggest that the preferred targets for indirect searches are the places with higher DM concentrations, like the centre of galaxies, satellites or galaxy clusters. It must be noticed however that the galactic centres are very often sources of strong activities due for example of the presence of black holes or other compact objects enhancing the overall background. Moreover the large uncertainty on the DM density profile directly reflects on the flux predictions making the searches extremely difficult (although possible enhancements due to local DM over-densities are possible).

DM particles can also generate high-energy photons. The Fermi satellite for example maybe able to indirectly detect DM particles looking at high energy photons. As example let us consider DM species at 40 GeV WIMP from a supersymmetric theory. That particle is supposed to annihilate into bottom-antibottom quark pairs. In this scenario, we show in the slide the flux map generated after five years of satellite operation. The map features the DM signal to noise ratio. The DM signal is the number of gamma rays produced towards each pixel by the DM distribution. The smooth DM distribution and the heaviest and closest DM substructures (bright spots on the maps), as expected in Λ CDM are considered.

The noise includes the galactic diffuse emission mostly arising from the interactions of cosmic rays protons and helium nuclei on the HI and H₂ gas components of the Milky Way. The two maps refer to different set of simulations: Aquarius (left panel) and Via Lactea II (right panel). It is then obvious how the DM density distribution in galaxies ρ_H plays a role, in particular, according whether in the innermost $R_{vir}/20$ region it is cuspy $\rho_H(r) \propto r^{-1}$ or constant. The predicted flux can differ by several orders of magnitude. Furthermore, one should also take into account the flux enhancements due to local DM over-densities i.e. sub-halo, but this is a very open question.

Another possibility is to pursue indirect search by looking at charged particles such as positrons or antiprotons, in this case however, the galactic magnetic field is such that the direction of arrival of the particle does not reflect the production point and the only observable is an excess of antimatter with respect to the expected background due to ordinary cosmic rays (which also suffer from big uncertainties).

Among the most important facilities for indirect signals we have: XMM Newton and Chandra, Integral, Compton Gamma Ray Observatory, AGILE, Fermi-LAT Observatory, CANGAROO, HESS, MAGIC, VERITAS, AMANDA, ICECUBE, ANTARES, PAMELA and AMS.

Up today several claims of indirect DM detection has been made, sometimes in conflict with each other and all of them competing with other astrophysical explanations, The most significant are: the positron excess measured by HEAT and PAMELA, the 511 keV line excess measured by INTEGRAL, the EGRET Diffuse Galactic Spectrum and the the so called WMAP Haze (an excess of microwave emission around the centre of the Milky Way) see Morselli (2010) for the current status on these searches. .

8 What we know?

Slides 69

The distribution of DM halos around galaxies shows a striking and complex phenomenology. We believe that it is giving invaluable information on the Nature itself of dark matter and on the galaxy formation processes.

Semi-analytical models as Baryon +DM simulations should reproduce the empirical scenario: a shallow DM inner distribution, strong relationships between the halo mass and 1) central halo density, 2) baryonic mass, 3) half-mass baryonic radius and 4) baryonic central surface density, a constant central halo surface density. In any case, the mass discrepancy in the World-Universe of galaxies is a

clear function of radius, total baryonic mass and Hubble Type

$$\frac{M_{grav}}{M_b} \sim \frac{1 + \gamma_1(M_b, T)r^3}{1 + \gamma_2(M_b, T)r^2}$$

that very unlikely may arise as effect of a change of the gravitation law.

References

- Aaronson, M. 1983, *ApJ*, 266, L11
- Bell, E. F. & de Jong, R. S. 2001, *ApJ*, 550, 212
- Belokurov, V., Zucker, D. B., Evans, N. W., et al. 2007, *ApJ*, 654, 897
- Bertone, G., Hooper, D., & Silk, J. 2005, *Phys. Rep.*, 405, 279
- Bosma, A. 1978, PhD thesis, PhD Thesis, Groningen Univ., (1978)
- Bosma, A. 1981a, *AJ*, 86, 1791
- Bosma, A. 1981b, *AJ*, 86, 1825
- Bosma, A. & van der Kruit, P. C. 1979, *A&A*, 79, 281
- Burkert, A. 1995, *ApJ*, 447, L25+
- Cappellari, M. 2008, *MNRAS*, 390, 71
- Cappellari, M., Bacon, R., Bureau, M., et al. 2006, *MNRAS*, 366, 1126
- Catinella, B., Giovanelli, R., & Haynes, M. P. 2006, *ApJ*, 640, 751
- Coccatto, L., Gerhard, O., Arnaboldi, M., et al. 2008, *Astronomische Nachrichten*, 329, 912
- Coccatto, L., Gerhard, O., Arnaboldi, M., et al. 2009, *MNRAS*, 394, 1249
- Conroy, C., Wechsler, R. H., & Kravtsov, A. V. 2006, *ApJ*, 647, 201
- Côté, P., Mateo, M., Olszewski, E. W., & Cook, K. H. 1999, *ApJ*, 526, 147
- de Blok, W. J. G., Walter, F., Brinks, E., et al. 2008, *AJ*, 136, 2648
- Donato, F., Gentile, G., Salucci, P., et al. 2009, *MNRAS*, 397, 1169
- Douglas, N. G., Arnaboldi, M., Freeman, K. C., et al. 2002, *PASP*, 114, 1234
- Ettori, S. & Fabian, A. C. 2006, *MNRAS*, 369, L42
- Fabricant, D., Rybicki, G., & Gorenstein, P. 1984, *ApJ*, 286, 186
- Freeman, K. C. 1970, *ApJ*, 160, 811
- Gargiulo, A., Haines, C. P., Merluzzi, P., et al. 2009, *MNRAS*, 397, 75
- Gentile, G., Burkert, A., Salucci, P., Klein, U., & Walter, F. 2005, *ApJ*, 634, L145
- Gentile, G., Salucci, P., Klein, U., Vergani, D., & Kalberla, P. 2004, *MNRAS*, 351, 903
- Gilmore, G., Wilkinson, M., Kleyna, J., et al. 2007a, *Nuclear Physics B Proceedings Supplements*, 173, 15
- Gilmore, G., Wilkinson, M. I., Wyse, R. F. G., et al. 2007b, *ApJ*, 663, 948
- Gnedin, O. Y., Kravtsov, A. V., Klypin, A. A., & Nagai, D. 2004, *ApJ*, 616, 16
- Governato, F., Brook, C., Mayer, L., et al. 2010, *Nature*, 463, 203
- Grillo, C., Gobat, R., Lombardi, M., & Rosati, P. 2009, *A&A*, 501, 461
- Hyde, J. B. & Bernardi, M. 2009, *MNRAS*, 396, 1171
- Jorgensen, I., Franx, M., & Kjaergaard, P. 1996, *MNRAS*, 280, 167
- Klypin, A., Trujillo-Gomez, S., & Primack, J. 2010, *ArXiv e-prints*

- Koopmans, L. V. E., Treu, T., Bolton, A. S., Burles, S., & Moustakas, L. A. 2006, *ApJ*, 649, 599
- Kormendy, J. & Freeman, K. C. 2004, in *IAU Symposium*, Vol. 220, *Dark Matter in Galaxies*, ed. S. Ryder, D. Pisano, M. Walker, & K. Freeman, 377–+
- Krajnović, D., Cappellari, M., Emsellem, E., McDermid, R. M., & de Zeeuw, P. T. 2005, *MNRAS*, 357, 1113
- Kuzio de Naray, R., McGaugh, S. S., & de Blok, W. J. G. 2008, *ApJ*, 676, 920
- Lapi, A. & Cavaliere, A. 2009, *ApJ*, 692, 174
- Mamon, G. A. & Lokas, E. L. 2005, *MNRAS*, 362, 95
- Mandelbaum, R., Seljak, U., Kauffmann, G., Hirata, C. M., & Brinkmann, J. 2006, *MNRAS*, 368, 715
- Mandelbaum, R., van de Ven, G., & Keeton, C. R. 2009, *MNRAS*, 398, 635
- Maraston, C. 1998, *MNRAS*, 300, 872
- Maraston, C. 2005, *MNRAS*, 362, 799
- Maraston, C., Daddi, E., Renzini, A., et al. 2006, *ApJ*, 652, 85
- Marinoni, C. & Hudson, M. J. 2002, *ApJ*, 569, 101
- Mateo, M. 1997, in *Astronomical Society of the Pacific Conference Series*, Vol. 116, *The Nature of Elliptical Galaxies; 2nd Stromlo Symposium*, ed. M. Arnaboldi, G. S. Da Costa, & P. Saha, 259–+
- Mateo, M. L. 1998, *ARA&A*, 36, 435
- Méndez, R. H., Teodorescu, A. M., Kudritzki, R., & Burkert, A. 2009, *ApJ*, 691, 228
- Mo, H. J., Mao, S., & White, S. D. M. 1998, *MNRAS*, 295, 319
- Morselli, A. 2010, *Mem. Soc. Astron. Italiana*, 81, 123
- Moster, B. P., Somerville, R. S., Maulbetsch, C., et al. 2010, *ApJ*, 710, 903
- Nagino, R. & Matsushita, K. 2009, *A&A*, 501, 157
- Napolitano, N. R., Arnaboldi, M., Freeman, K. C., & Capaccioli, M. 2001, *A&A*, 377, 784
- Napolitano, N. R., Romanowsky, A. J., Capaccioli, M., et al. 2010, *MNRAS*, 1835
- Navarro, J. F., Frenk, C. S., & White, S. D. M. 1997, *ApJ*, 490, 493
- Oh, S., de Blok, W. J. G., Walter, F., Brinks, E., & Kennicutt, R. C. 2008, *AJ*, 136, 2761
- Persic, M., Salucci, P., & Stel, F. 1996, *MNRAS*, 281, 27
- Plummer, H. C. 1915, *MNRAS*, 76, 107
- Rubin, V. C., Peterson, C. J., & Ford, Jr., W. K. 1980, *ApJ*, 239, 50
- Salucci, P., Lapi, A., Tonini, C., et al. 2007, *MNRAS*, 378, 41
- Salucci, P., Nesti, F., Gentile, G., & Frigerio Martins, C. 2010, *A&A*, 523, A83+
- Schneider, P. 1996, *MNRAS*, 283, 837
- Schneider, P., Kochanek, C. S., & Wambsganss, J., ed. 2006, *Weak Gravitational Lensing* (Springer-Verlag), 269–+
- Shankar, F. & Bernardi, M. 2009, *MNRAS*, 396, L76
- Shankar, F., Lapi, A., Salucci, P., De Zotti, G., & Danese, L. 2006, *ApJ*, 643, 14
- Spano, M., Marcelin, M., Amram, P., et al. 2008, *MNRAS*, 383, 297

- Strigari, L. E., Bullock, J. S., Kaplinghat, M., et al. 2008, *Nature*, 454, 1096
- Tinsley, B. M. 1975, *Mem. Soc. Astron. Italiana*, 46, 3
- Tiret, O., Salucci, P., Bernardi, M., Maraston, C., & Pforr, J. 2010, *MNRAS*, 1737
- Trachternach, C., de Blok, W. J. G., Walter, F., Brinks, E., & Kennicutt, R. C. 2008, *AJ*, 136, 2720
- Tully, R. B. & Fisher, J. R. 1977, *A&A*, 54, 661
- Vale, A. & Ostriker, J. P. 2004, *MNRAS*, 353, 189
- Walker, M. G., Mateo, M., Olszewski, E. W., et al. 2007, *ApJ*, 667, L53
- Walker, M. G., Mateo, M., Olszewski, E. W., et al. 2009, *ApJ*, 704, 1274
- Walker, M. G., Mateo, M., Olszewski, E. W., et al. 2010a, *ApJ*, 710, 886
- Walker, M. G., McGaugh, S. S., Mateo, M., Olszewski, E. W., & Kuzio de Naray, R. 2010b, *ApJ*, 717, L87
- Wechsler, R. H., Bullock, J. S., Primack, J. R., Kravtsov, A. V., & Dekel, A. 2002, *ApJ*, 568, 52
- Wechsler, R. H., Zentner, A. R., Bullock, J. S., Kravtsov, A. V., & Allgood, B. 2006, *ApJ*, 652, 71
- Wilkinson, M. I., Kleyna, J. T., Wyn Evans, N., et al. 2006, in *EAS Publications Series*, Vol. 20, *EAS Publications Series*, ed. G. A. Mamon, F. Combes, C. Deffayet, & B. Fort, 105–112
- Willman, B., Blanton, M. R., West, A. A., et al. 2005, *AJ*, 129, 2692
- Wolf, J., Martinez, G. D., Bullock, J. S., et al. 2010, *MNRAS*, 406, 1220
- Wong, T. & Blitz, L. 2002, *ApJ*, 569, 157
- Yegorova, I. A. & Salucci, P. 2007, *MNRAS*, 377, 507

A APPENDIX DMAW 2010 Seminar Speakers

Speaker	Institute	City	Nation
S. AL-Jaber	An-Najah National University	Nablus	Palestine
J. Aleksic	Institut de Fisica d'Altes Energies	Bellaterra	Spain
G. Alves Silva	Universidade Estadual de Roraima	Boa Vista	Brasil
J. Bailin	University of Michigan	Ann Arbor	USA
M. Balcells	Isaac Newton Group of Telescopes	La Palma	Spain
M. Baldi	Excellence Cluster Universe	Garching	Germany
G. Barbiellini	INFN Trieste	Trieste	Italy
N. Bartolo	Physics Department "Galileo Galilei", University of Padova & INFN Padova	Padova Padova	Italy Italy
M. Bastero Gil	University of Granada	Granada	Spain
G. K. Beeharry	Mauritius Radio Telescope, University of Mauritius	Reduit	Mauritius
Bernal, Degollado, Hidalgo, Barranco & Mastache	Universidad Nacional Autonoma de Mexico	Mexico City	Mexico
M. Bernardi	University of Pennsylvania	Philadelphia	USA
O. Bertolami	University of Porto	Porto	Portugal
N. Bilic	Rudjer Boskovic Institute University of Zagreb	Zagreb Zagreb	Croatia Croatia
S. Bird	University of Turku	Turku	Finland
A. Biviano	Osservatorio Astronomico di Trieste	Trieste	Italy
C. Böehmer	Institute of Origins, University College London	London	UK
A. Bosma	Beijing Normal University & Laboratoire d'Astrophysique de Marseille	Beijing Marseille	China France
F. Bournaud	CEA Saclay	Saclay	France
H. Bray & A. Badin	Duke University	Durham	USA
A. Bressan	Osservatorio Astronomico di Padova & Dept. Astronomy	Padua	Italy
I. Brown	University of Oslo	Oslo	Norway
D. Cabral Rodrigues	Universidade Federal do Espírito Santo	Vitória	Brazil
S. Capozziello	Università di Napoli "Federico II"	Naples	Italy
L. Caramete & P. Stefanescu	Institute for Space Sciences	Bucharest-Magurele	Romania
B. Cervantes-Sodi	Korea Astronomy & Space Science Institute	Daejeon	Korea
R. Chavez	INAOE Instituto Nacional de Astrofisica Optica y Electronica	Puebla	Mexico
L. Chemin	Laboratoire d'Astrophysique de Bordeaux	Floirac	France
P. Chimenti	UFABC Universidade Federal do ABC	Santo André	Brazil
S. Colafrancesco	Osservatorio Astronomico di Roma & Università di Roma La Sapienza	Roma Roma	Italy Italy
L.P. Colatto	CEFET Petrópolis	Petrópolis	Brazil
C. Collins	Liverpool John Moores University	Merseyside	UK
M. Colpi	University of Milano Bicocca, Physics Dept. G. Occhialini	Milan	Italy
G. Dastagir Al-Quaderi	University of Dhaka	Dhaka	Bangladesh
R. Dave	Raman Research Institute	Bangalore	India
R. de Grijs	Kavli Institute for Astronomy & Astrophysics, Peking University	Beijing	China
F. De Paolis	University of Salento	Lecce	Italy
A. Del Popolo	Catania University	Catania	Italy
S. di Serego Alighieri	Osservatorio Astrofisico di Arcetri	Florence	Italy
A. Erkurt	University of the Basque Country	Bizkaia	Spain
M. Fairbairn	King's College	London	UK
B. Famaey	Observatoire Astronomique de Strasbourg	Strasbourg	France
V. Faraoni	Bishop's University	Sherbrooke	Canada
R. Fisher	UMass Dartmouth	North Dartmouth	USA
P. Flin & J. Jalocha Bratek	Jan Kochanowski University	Kielce	Poland
C. Flynn	University of Sydney	Sydney	Australia
C. Frigerio Martins	Universidade Estadual de Campinas UNICAMP	Campinas	Brasil
F. Frutos-Alfaro	Space Research Center, University of Costa Rica	San José	Costa Rica
J. Funes	Specola Vaticana	Vatican	Vatican
P. Galianni	University of St Andrews	St Andrews	UK
J. Gan	Shanghai Astronomical Observatory	Shanghai	China
G. Gentile	Katholieke Universiteit Leuven & Vrije Universiteit Brussel	Leuven Brussels	Belgium Belgium
I. George	University Maryland Baltimore County	Baltimore County	USA
S. George	University of Calgary	Calgary	Canada
L.Á. Gergely & M. Dwornik	University of Szeged	Szeged	Hungary
M. Gomez	Universidad de Huelva	Huelva	Spain
P. Gondolo	University of Utah	Salt Lake City	USA
M. Goto	Universidade Estadual de Londrina	Londrina	Brazil
M. Grossi	University of Lisbon	Lisbon	Portugal
L. T. Handoko	Indonesian Institute of Sciences	Tangerang	Indonesia
T. Harko	The University of Hong	Hong Kong	China

N. Hashim, M.S.R. Hassan & I. Ungu	University of Malaya, Radio Cosmology Research Lab.	Kuala Lumpur	Malaysia
M. Hendry	University of Glasgow	Glasgow	UK
F. Hessman	University of Goettingen	Göttingen	Germany
S. Horvath	University of Canterbury	Christchurch	New Zealand
D. Iakubovskiy	Bogolyubov Institute for Theoretical Physics	Kiev	Ukraine
C. Impey	University of Arizona	Tucson	USA
C. Kilinc	Ege University	Izmir	Turkey
S. Kim	Kyung Hee University	Seoul	South Korea
D. Kirilova & G. Petrov	Bulgarian Academy of Sciences, Institute of Astronomy	Sofia	Bulgaria
A. Knebe	Universidad Autonoma de Madrid	Madrid	Spain
S. Knollmann	University of Zaragoza	Zaragoza	Spain
A. Lalovic & S. Samurovic	Astronomical Observatory in Belgrade	Belgrade	Serbia
A. Lapi	University of Rome "Tor Vergata"	Rome	Italy
B. Lazartot Lago	CEFET Nova Friburgo	Nova Friburgo	Brazil
R. Machado	IAG Universidade de São Paulo	São Paulo	Brazil
D. Makarov	Russian Academy of Sciences	Zelenchuck	Russia
A. Maller	The New York City College of Technology	New York	USA
G. Mamon	Institut d'Astrophysique de Paris	Paris	France
D. Manreza Paret & E. Rodriguez Querts	Universidad de La Habana	La Habana	Cuba
C. Maraston	Institute of Cosmology and Astrophysics	Portsmouth	UK
D. Marchesini	Tufts University	Medford	USA
C. Martins	Centro de Astrofísica da Universidade do Porto	Porto	Portugal
T. Matos	Cinvestav	Mexico City	Mexico
T. Matos	Instituto de Física y Matemáticas de la Universidad Michoacana	Morelia	Mexico
A. Meza	Universidad Andrés Bello	Santiago	Chile
S. Mohanty	Physical Research Laboratory	Ahmedabad	India
M. Molla	Centro de Investigaciones Energéticas, Medioamb. y Tecnol.	Madrid	Spain
J. C. Muñoz Cuartas	Astrophysikalisches Institut Postdam	Potsdam	Germany
S. Murgia, L. Strigari & R. Wechsler	KIPAC, SLAC, Stanford University	Stanford	USA
K. Nagamine	University of Nevada	Las Vegas	USA
N. Napolitano	Astronomical Observatory of Capodimonte	Naples	Italy
D. Nieto Castaño & J.A. Ruz Cembranos	Complutense University of Madrid	Madrid	Spain
F. Nesti	INFN Laboratori Nazionali del Gran Sasso	L'Aquila	Italy
A. Ogulenko	Odessa I.I. Mechnikov National University	Odessa	Ukraine
Á. Orsi	Universidad Católica de Chile	Santiago	Chile
N. Padilla	Universidad Católica de Chile	Santiago	Chile
A. Parnowski	Space Research Institute National Academy of Sciences	Kyiv	Ukraine
A. Parnowski	Kyiv Taras Shevchenko National University	Kyiv	Ukraine
P. Patsis	Academy of Athens, Research Center for Astronomy	Athens	Greece
V. Pettorino	Fourth TRR33 Winter School	Passo del Tonale	Italy
M. Plionis	National Observatory of Athens, Inst. Astron. & Astrophys.	Athens	Greece
J. Polednikova	Faculty of Science, Masaryk University	Moravia	Czech Republic
L. Reverberi	University of Ferrara	Ferrara	Italy
M. D. Rodriguez Frias	University of Alcalá	Alcalá de Henares	Spain
A. Romeo	Onsala Space Observatory, Chalmers	Onsala	Sweden
R. Rosenfeld	Unesp Instituto de Física Teórica	São Paulo	Brazil
M. Roos	University of Helsinki & University of Helsinki- Astrophysics Group	Helsinki Helsinki	Finland Finland
A. Saburova & A. Zasov	Sternberg Astronomical Institute	Moscow	Russia
P. Salucci	Observatory of Bologna SISSA	Bologna Trieste	Italy Italy
M. Sanchez-Conde	Instituto de Astrofísica de Canarias	La Laguna	Spain
K. Sapountzis & M. Petropoulou	National & Kapodistrian University of Athens	Athens	Greece
M. Schneider	Lawrence Livermore National Laboratory	Livermore	USA
S. Schulze	University of Iceland, Centre for Astrophysics and Cosmology	Dunhagi	Iceland
D. Schwarz & M. Stuke	Universitaet Bielefeld	Bielefeld	Germany
M. Seigar	University of Arkansas at Little Rock	Little Rock	USA
N. Seymour	Mullard Space Science Laboratory, University College London	Dorking	UK
M. D. Sheppard	Victoria University of Wellington	Wellington	New Zealand
Y-S.Song	Korea Institute for Advanced Study	Seoul	Korea
C. Struck	Iowa State University	Ames	USA
G. Tadaiesky Marques	Universidade Federal do Pará	Belém	Brazil
A. Tartaglia	Politecnico di Torino, DIFIS	Torino	Italy
A. N. Tawfik	Egyption Center for Theoretical Physics	Cairo	Egypt
P. Thomas	University of Sussex	Sussex	UK

P. Tissera	Institute for Astronomy and Space Physics	Buenos Aires	Argentina
C. Tonini	University of Melbourne	Melbourne	Australia
L.A. Urena-Lopez	University of Guanajuato, Physics Dept.	Guanajuato	Mexico
J. van Eymeren	Universitaet Duisburg-Essen & Ruhr University Bochum	Duisburg Bochum	Germany Germany
A. Velsquez-Toribio	Universidade Federal de Juiz de Fora	Juiz de Forma	Brazil
M. Viel	ICTP	Trieste	Italy
A. Vincent	McGill University	Montreal	Canada
A-M. Weijmans & V. Sanz	York University, Dept. Physics & Astronomy	York	Canada
R. Wojtak	Dark Cosmology Centre	Copenhagen	Denmark
N. Yamasaki	Institute of Space & Astronautical Science	Chofu	Japan
F. Zandanel	Instituto de Astrofisica de Andalucia	Granada	Spain
B. Ziegler	University of Vienna	Vienna	Austria

DARK MATTER IN GALAXIES

NAME
INSTITUTE

Outline of the Review

Dark Matter is main protagonist in the Universe

This review focus: Dark Matter in Galaxies

The concept of Dark Matter in virialized objects
 Dark Matter in Spirals, Ellipticals, dSphs
 Dark and Luminous Matter in galaxies. Global properties.
 Phenomenology of the mass distribution in Galaxies.
 Implications for Direct and Indirect Searches

3 MAJOR TYPES OF GALAXIES

spiral
elliptical
dwarfs

The Realm of Galaxies

The range of galaxies in magnitudes, types and central surface densities: 15 mag, 4 types, 16 mag arcsec⁻²

Central surface brightness vs galaxy magnitude

The distribution of luminous matter:
 Spirals: stellar disk + bulge + HI disk
 Ellipticals & dwarfs: E: stellar spheroid

What is Dark Matter ?

In a galaxy, the radial profile of the gravitating matter $M(r)$ does not match that of the luminous component $M_l(r)$.

A MASSIVE DARK COMPONENT is then introduced to account for the disagreement: its profile $M_d(r)$ must obey:

$$\frac{d \log M(r)}{d \log r} = \frac{M_l(r)}{M(r)} \frac{d \log M_l(r)}{d \log r} + \frac{M_d(r)}{M(r)} \frac{d \log M_d(r)}{d \log r}$$

$M(r)$, $M_l(r)$, $d \log M_l(r)/d \log r$ observed

The DM phenomenon can be investigated only if we accurately measure the distribution of:
 Luminous matter $M_l(r)$
 Gravitating matter $M(r)$

THEORY AND SIMULATIONS

ΛCDM Dark Matter Density Profiles from N-body simulations

The density of virialized DM halos of any mass is empirically described at all times by an Universal profile (Navarro+96, 97, NFW).

$$\rho_{NFW}(r) = \delta \rho_0 \frac{r_s}{r} (1 + r/r_s)^{-2}$$

$$c = \frac{R_{vir}}{r_s} \quad R_{vir} = 200 \left(\frac{M_{vir}}{10^{12} M_\odot} \right)^{1/3} \text{ kpc}$$

More massive halos and those formed earlier have larger overdensities
 Today mean halo density inside $R_{vir} = 100 \rho_c$
 $c(M_{vir}) = 9.36 \left(\frac{M_{vir}}{10^{12} M_\odot} \right)^{-0.69}$ Klypin, 2010

Aquarius N-Body simulations, highest mass resolution to date.

Density distribution: the Einasto Law indistinguishable by NFW

How halos form and evolve

SPIRALS

Stellar Disks

M33 disk very smooth, truncated at 4 scale-lengths
 NGC 300 exponential disk for at least 10 scale-lengths

$$I(r) = I_0 e^{-r/R_D}$$

Freeman, 1970
 R_D length scale of the disk

Gas surface densities

HI
 Flattish radial distribution
 Deficiency in the centre
 Extended to $(8-40) R_D$

H₂
 Follows the stellar disk
 Negligible

Circular velocities from spectroscopy

- Optical emission lines (H α , H β)
- Neutral hydrogen (HI)-carbon monoxide (CO)

Tracer	angular resolution	spectral resolution
HI	7" ... 30"	2 ... 10 km s ⁻¹
CO	1.5" ... 8"	2 ... 10 km s ⁻¹
H α , ...	0.5" ... 1.5"	10 ... 30 km s ⁻¹

ROTATION CURVES

Longer arrows represent larger orbital velocities.

Copyright © Andrian Winkler

Figure 1: Zoomed out slides of the Presentation Review, shown here to give a glimpse of it. These slides can be downloaded at http://www.sissa.it/ap/dmg/dmaw_presentation.html

16

Symmetric circular rotation of a disk characterized by

- Sky coordinates of the galaxy centre
- Systemic velocity V_{sys}
- Circular velocity $V(R)$
- Inclination angle

UGC2405 HIGH QUALITY ROTATION CURVE

17

Early discovery from optical and HI RCs

RC DO NOT FOLLOWS THE DISK VELOCITY PROFILE

Robinet 1780

MASS DISCREPANCY AT OUTER RADII

18

HI rotation curves beyond the optical image

Bosma, 1978, 1981a,b

Robota, 1978; Bosma & Van der Kruit 1979

19

Evidence for a Mass Discrepancy in Galaxies

The distribution of gravitating matter, unlike the luminous one, is luminosity-independent.

Tully-Fisher relation exists at local level (radii R_1)

no DM

Yegorov et al. 2012

20

Rotation Curves

Coadded from 3200 individual RCs

TYPICAL INDIVIDUAL RCs OF INCREASING LUMINOSITY

21

The Cosmic Variance of V measured in galaxies of same luminosity L at the same radius $x=R/R_0$ is negligible compared to the variations that V shows as x and L varies.

The Universal Rotation Curve

22

Universal Rotation Curve out to the Virial Radius

Method: inner kinematics + independent determinations of halo vital masses

Virial masses M_v of halos around galaxies with stellar mass M_{star} (or luminosity L) are obtained

- directly by weak-lensing analysis (left)
- indirectly by correlating dV/dL with theoretical DM halo dM/dL (right)

23

The Concept of the Universal Rotation Curve (URC)

Every RC can be represented by: $V(x,L) = R/R_0$

The URC out to $4 R_0$ is derived directly from observations. Extrapolation of URC out to virial radius by using $V(R_{vir})$.

-> Movie 2

24

Rotation curve analysis

From data to mass models

$$V^2(R) = V_{disk}^2(R) + V_{HI}^2(R) + V_{dark}^2(R)$$

observations =

- V_{disk}^2 from I-band photometry
- V_{HI}^2 from HI observations
- V_{dark}^2 different choices for the DM halo density

Dark halos with central constant density (Burkert, Isothermal)

Dark halos with central cusps (NFW, Einasto)

The mass model has 3 free parameters: disk mass, halo central density, halo core radius (length-scale). Obtained by best fitting method.

25

MASS MODELLING RESULTS

All structural DM and LM parameters are related with luminosity.

Smaller galaxies are denser and have a higher proportion of dark matter.

26

Dark Halo Scaling Laws in Spirals

Careful investigation of relationships between halo structural parameters and luminosity, via mass modelling of individual galaxies (ρ_0, r_0)

- Assumption: Maximum Disk, 30 objects
- the central slope of the halo rotation curve gives the halo core density
- extended RCs provide an estimate of halo core radius: r_0

Central Density vs Abs. Mag. vs Core Radius vs Abs. Mag.

URC

$\rho_0 \sim L^{-0.7}$

$r_0 \sim L^{0.7}$

$\rho_0 \sim L^{-0.6}$

$r_0 \sim L^{0.6}$

27

The halo central surface density $\rho_0 r_0$: constant in Spirals

$\rho_0 r_0 \propto L^{0.021 \pm 0.027}$

Kormendy & Freeman (2004)

28

The distribution of DM around spirals

Using individual galaxies: Gentile+2006, de Blok+2008, Kuzio de Naray+2008, Oh+2008, Spano+2008, Trachternach+2008, Donato+2009

A detailed investigation: high quality data and model independent analysis

Galaxy Dynamics in THINGS — The HI Nearby Galaxy Survey

29

EXAMPLES

IC 2574

DDO 47

General results from several samples e.g. THINGS

- Non-circular motions are small.
- DM halo spherical
- ISO/Burkert halos much more preferred over NFW
- Tri-axial and non-circular motions cannot explain the CDM/NFW cusp/core discrepancy

30

SPIRALS: WHAT WE KNOW

AN UNIVERSAL CURVE REPRESENTS ALL INDIVIDUAL RCs


MORE PROPORTION OF DARK MATTER IN SMALLER SYSTEMS

THE RADIUS IN WHICH THE DM SETS IN IS A FUNCTION OF LUMINOSITY

THE MASS PROFILE AT LARGER RADII IS COMPATIBLE WITH NFW

DARK HALO DENSITY SHOWS A CENTRAL CORE OF SIZE $2 R_0$

ELLIPTICALS



The Stellar Spheroid

Surface brightness of ellipticals follows a Sérsic (de Vaucouleur)

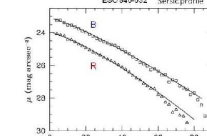
$$I(R) = I_e \left[\exp\left(-b_e \left(\frac{R}{R_e}\right)^{1/n}\right) - 1 \right]^{-n}$$

$b_e = 0.868 n - 0.112$ R_e the radius enclosing half of the projected light

By deprojecting $I(R)$ we obtain the luminosity density $j(r)$:

$$I(R) = \int_{-\infty}^{\infty} j(r) dz = 2 \int_0^R \frac{j(r) r dr}{\sqrt{R^2 - r^2}}$$

$\rho_{sph}(r) = (M/L) * j(r)$



Modelling Ellipticals

Measure the light profile = stellar mass profile $(M_*/L)^{-1}$

Derive the total mass profile $M(r)$

- Dispersion velocities of stars or Planetary Nebulae
- X-ray properties of the emitting hot gas
- Weak and/or strong lensing data

Disentangle $M(r)$ into its dark and the stellar components

In ellipticals gravity is balanced by pressure gradients -> Jeans Equation

$$\frac{d}{dr} (\rho \sigma^2) + \frac{2\rho}{r} \sigma^2 = -\rho \frac{d\Phi}{dr} \rightarrow \text{grav. potential}$$

dispersion velocities

Kinematics of ellipticals: Isotropic Jeans modelling of velocity dispersions

$M(r) = M_*(r) + M_D(r)$

$\sigma^2(r) = \frac{G}{2\pi a(r)} \int_0^a \frac{\rho_{sph}(r') M(r')}{r'^2} dr'$ radial not observable

$\sigma^2(r) = \frac{2}{\pi} \int_0^a \frac{\rho_{sph}(r') \sigma^2(r')}{\sqrt{a^2 - r'^2}} r' dr'$ projected

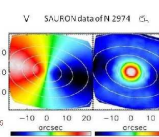
$\sigma^2(R) = \frac{2\pi}{L(R)} \int_0^R \rho_{sph}(r) I(r) R dr$ aperture

$L(R) = 2\pi \int_0^R I(r) R dr$

measure $I(R)$, $\sigma_p(R)$
derive $M_*(R)$, $M_{DM}(R)$
Rotation is not always negligible

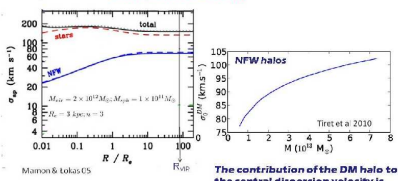
Anisotropic Jeans equations

$$\frac{\partial}{\partial R} \left(\rho \sigma^2 \right) + \frac{\partial}{\partial z} \left(\rho \sigma_z^2 \right) + \nu \left(\frac{\partial \sigma^2}{\partial R} - \frac{\partial \sigma_z^2}{\partial R} \right) = 0$$

$$\frac{\partial}{\partial R} \left(\rho \sigma^2 \right) + \frac{\partial}{\partial z} \left(\rho \sigma_z^2 \right) + \nu \frac{\partial \Phi}{\partial R} = 0$$


Warning: mass decomposition of dispersion velocities not unique.

Example: NFW halo + Sérsic spheroid, Orbit isotropy.



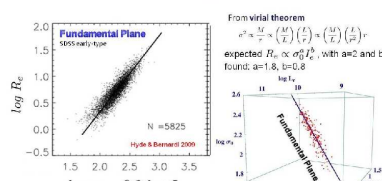
$M_{DM} = 2 \times 10^{12} M_\odot, M_{DM} = 1 \times 10^{13} M_\odot$
 $\sigma_{DM} = 3 \text{ km/s} = 3$

Tiret et al 2010

The contribution of the DM halo to the central dispersion velocity is lesser than 100 km/s

Inside R_e the dark matter profile is intrinsically unresolvable

The Fundamental Plane: the values of the central dispersion velocity, half light radius and central surface brightness are strongly related



$\log R_e$ vs $\log \sigma_0 - 0.2 \log I_e$


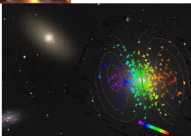
From virial theorem $\sigma^2 \sim \frac{M}{r} \left(\frac{L}{r} \right) \sim \left(\frac{M}{r} \right) \left(\frac{L}{r} \right)$
expected $R_e \propto \sigma_0^2 I_e^{-1}$ with $a=2$ and $b=1$
found: $a=1.8$, $b=0.6$

FP "tilt" due to variations with σ_0 of Stellar populations among E

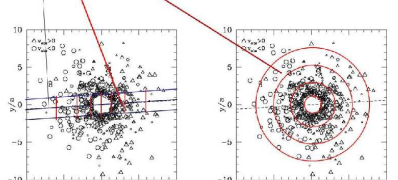
Jorgensen et al 1990

The Planetary Nebula Spectrograph

Extended kinematics of elliptical galaxies obtained with the Planetary Nebula Spectrograph

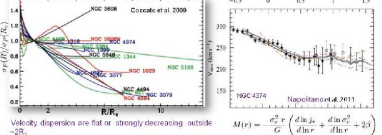



Major/minor axis or radial binning of the data

$$\sigma_r = \frac{1}{N-1} \sum_{i=1}^N (v_i - \bar{v})^2$$


PN data

Jeans modelling of PN data with a stellar spheroid + NFW dark halo



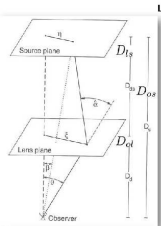
Velocity dispersions are flat or strongly decreasing outside

$M(r) = \frac{\sigma^2 r}{G} \left(\frac{d \ln L}{d \ln r} + \frac{d \ln \sigma^2}{d \ln r} - 2 \right)$

JEANS ANALYSIS
There exist big DM halos around Ellipticals. Cores and cuspy DM profiles are both possible.
MORE DATA

Mass profiles from weak lensing

Lensing equation for the observed tangential shear e.g. Schneider, 1996



$$\gamma_t = \frac{\Sigma(R) - \Sigma(R)}{\Sigma_e(R)}$$

$$\Sigma = \frac{M(R)}{4\pi R^2}$$

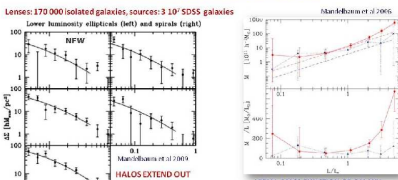
$$R = \theta D_{OL}$$

$$\frac{\gamma_t}{\Sigma_e} = \frac{\sigma^2 D_{OL}}{4\pi G D_{OL} D_{OS}}$$

MODELLING WEAK LENSING SIGNALS

Lenses: 170 000 isolated galaxies, sources: 3 10⁵ SDSS galaxies

Lower luminosity ellipticals (left) and spirals (right)



HALOS EXTEND OUT TO VIRIAL RADI

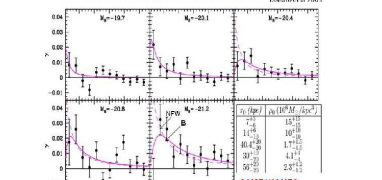
Virial mass function of galaxy luminosity

Halo masses exceed the masses in baryons by much more than the cosmological factor of 7.

Halo and baryonic masses correlate.

OUTER DM HALOS: NFW/BURKERT PROFILE FIT THEM EQUALLY WELL

Reichert et al 2005



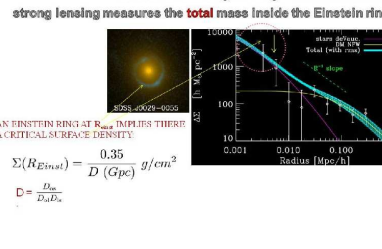
Same values found by mass modelling the URC

Weak and strong lensing

strong lensing measures the total mass inside the Einstein ring

AN EINSTEIN RING AT R_{EIN} IMPLIES THERE A CRITICAL SURFACE DENSITY

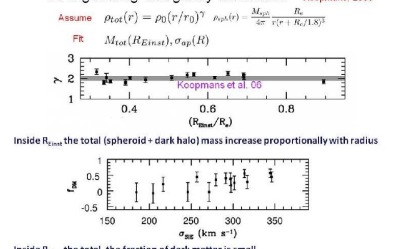
$$\Sigma(R_{EIN}) = \frac{0.35}{D(Gpc)} g/cm^2$$

$$D = \frac{D_{OL} D_{OS}}{D_{OS}}$$


Strong lensing and galaxy kinematics

Assume $\rho_{tot}(r) = \rho_0(r/r_0)^{-\alpha}$ $\rho_{tot}(r) = \frac{M_{tot}}{4\pi r^2 (r/r_0)^{3-\alpha}}$

FR $M_{tot}(R_{EIN}) = \sigma_{app}(R)$

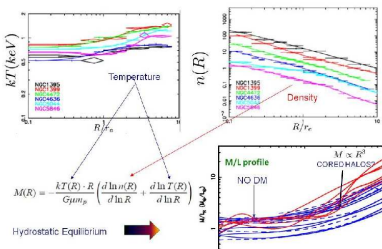


Inside R_{EIN} the total (spheroid + dark halo) mass increase proportionally with radius

Inside R_{EIN} the total the fraction of dark matter is small

Mass Profiles from X-ray

Nijboer et al 2009



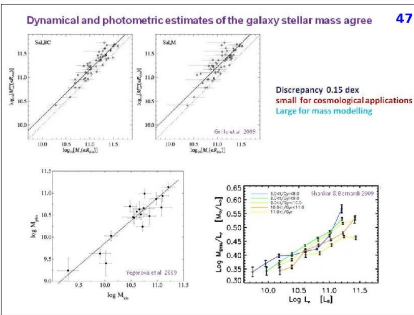
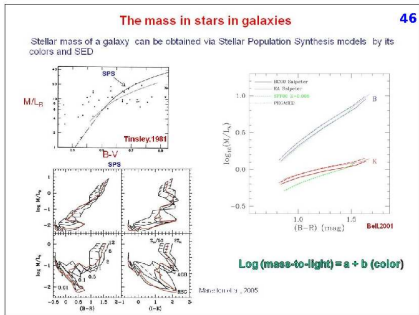
Hydrostatic Equilibrium

$M(r) = \frac{kT(r) \cdot R}{G \mu m_p} \left(\frac{d \ln n(R)}{d \ln R} + \frac{d \ln T(R)}{d \ln R} \right)$

M/L profile

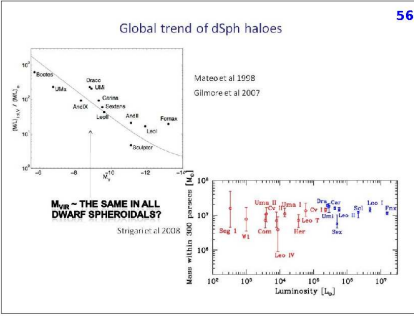
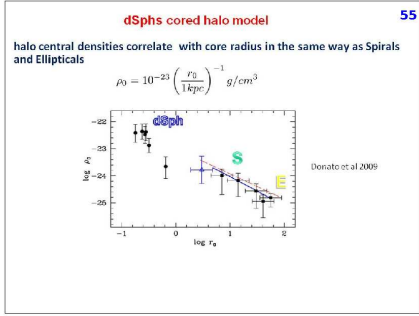
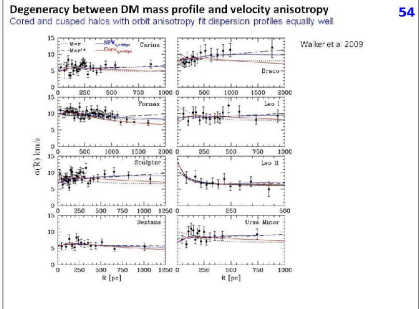
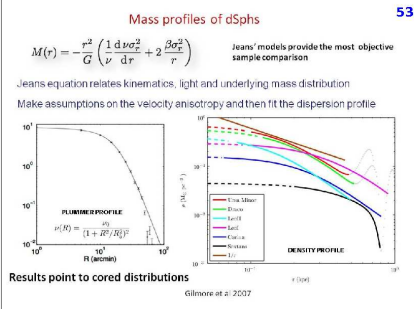
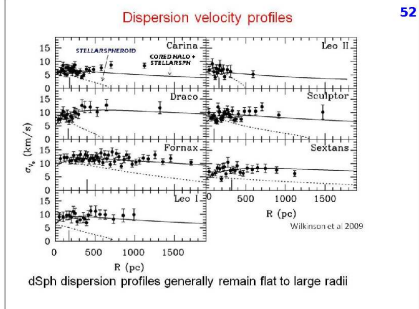
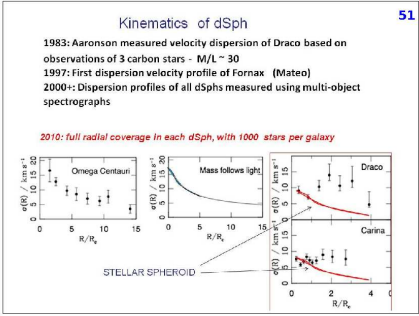
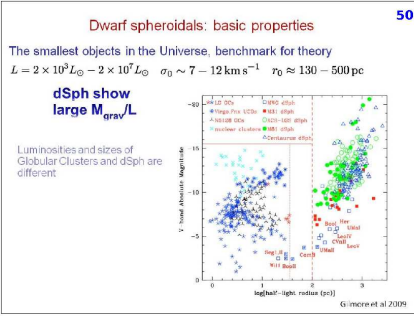
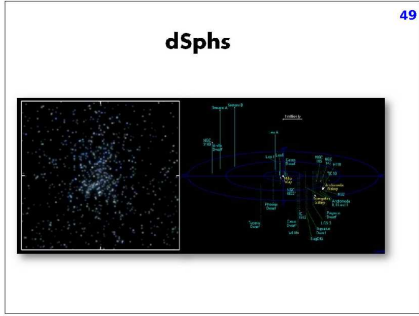
NO DM

$M/L \propto R^2$ CORED HALOS



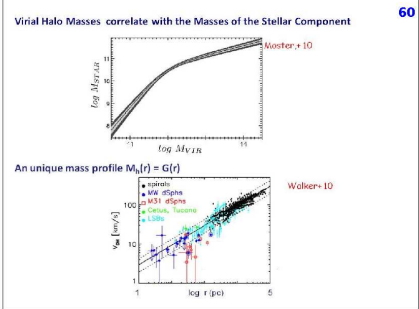
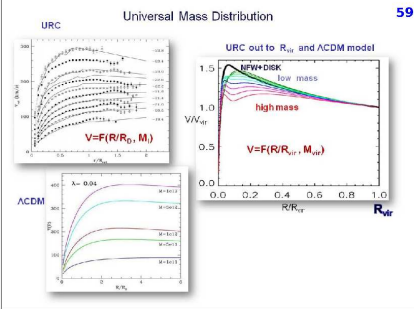
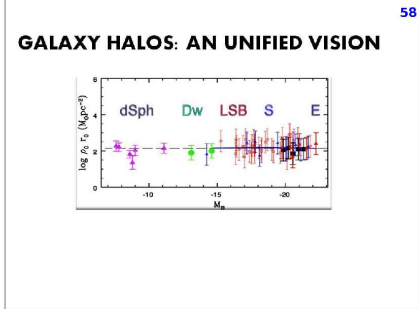
ELLIPTICALS: WHAT WE KNOW

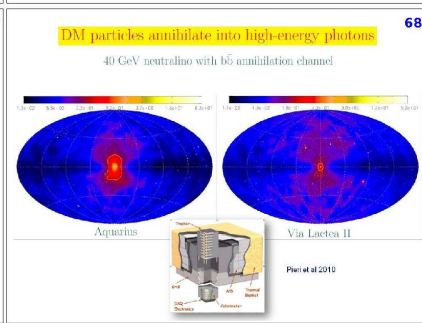
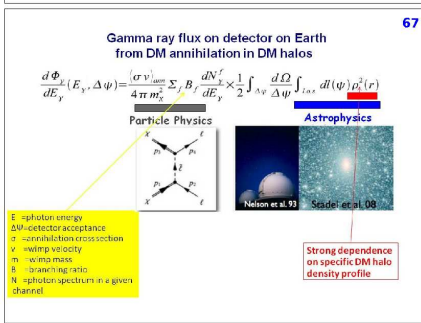
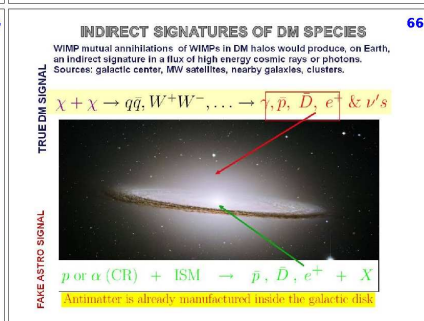
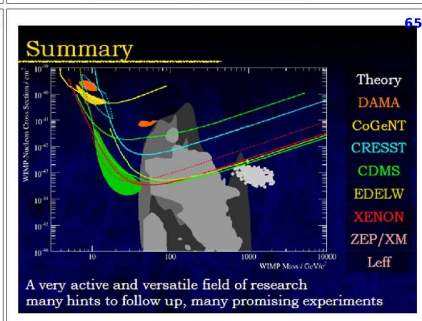
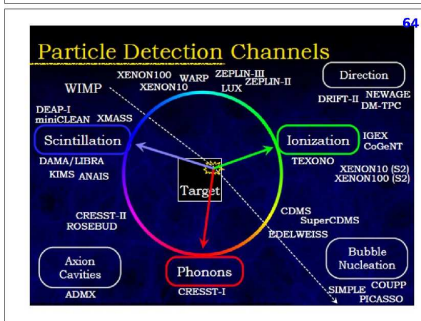
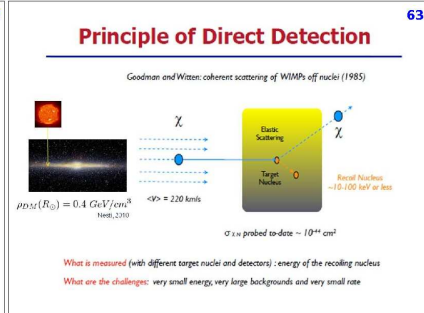
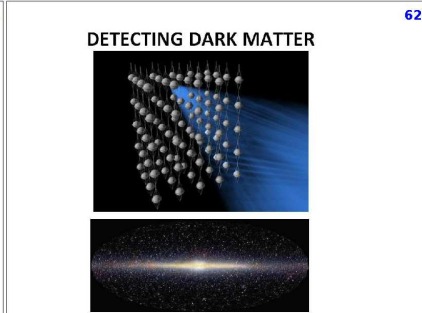
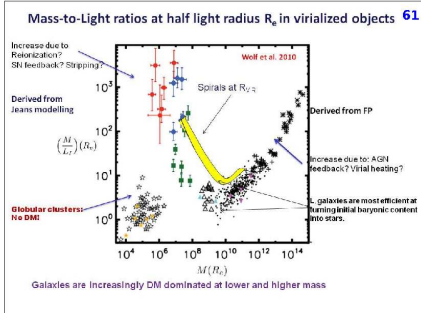
A LINK AMONG THE STRUCTURAL PROPERTIES OF STELLAR SPHEROID SMALL AMOUNT OF DM INSIDE R_e MASS PROFILE COMPATIBLE WITH NFW AND BURKERT DARK MATTER DIRECTLY TRACED OUT TO R_{vir}



DSPH: WHAT WE KNOW

PROVE THE EXISTENCE OF DM HALOS OF $10^{10} M_{\odot}$ AND $\rho_0 = 10^{-21} \text{ g/cm}^3$ DOMINATED BY DARK MATTER AT ANY RADII MASS PROFILE CONSISTENT WITH THE EXTRAPOLATION OF THE URC HINTS FOR THE PRESENCE OF A DENSITY CORE





WHAT WE KNOW? 69

The distribution of DM in halos around galaxies shows a striking and complex phenomenology crucial to understand

The nature of dark matter and the galaxy formation process
Refined simulations should reproduce and the theory should explain:

- a shallow DM inner density distribution, a central halo surface density independent of halo mass and a series of relationships between the latter and the i) central halo density, ii) baryonic mass, iii) half-mass baryonic radius and iv) baryonic central surface density

Theory, phenomenology, simulations, experiments are all bound to play a role in the search for dark matter and its cosmological role.

The mass discrepancy in galaxies is a complex function of radius, total baryonic mass, Hubble Type

$$\frac{M_{grav}}{M_b} = 1 + \eta_1 (M_b, T)^{\eta_2}$$

Unlikely all this masks a new law of Gravity but certainly it is beyond the present Λ CDM predictive power

This Presentation has been prepared by:
Paolo Salucci, Christiane Frigerio Martins, Andrea Lapi
 with the scientific collaboration of:
 Eleno Aprile, Mariangela Bernardi, Albert Bosma, Erwin de Blok, Ken Freeman, Rafael Gavazzi, Gianfranco Gentile, Gerry Gilmore, Uli Klein, Gary Mamon, Claudia Maraston, Nicola Napolitano, Pierre Salati, Chiara Tonini, Mark Wilkinson, Irina Yegorova.
 with the support and encouragement of:
 J. Balin, P. Biermann, A. Bressan, L. Danese, C. Frenk, S. Leach, M. Roos, V. Rubin.

If you play it, it will be also yours!
 If you deliver it, it will become yours!

Thanks to everyone!

Figure 2: Zoomed out slides of the Presentation Review, shown here to give a glimpse of it. These slides can be downloaded at http://www.sissa.it/ap/dmg/dmaw_presentation.html